Ministry of Higher Education and Scientific Research

وزارة التعليم العالي و البحث العلمي

Badji Mokhtar Annaba University
Université Badji Mokhtar – Annaba
Faculty of technology
Electromechanical department

جامعة باجي مختار – عنابـــــــــة

كلية التكنولوجيا
قســـــــم الالكتروميكانيك

Thesis

Presented to obtain the diploma of

Doctorate

Specialty: Industrial maintenance

Field: Electromechanics

By:

BEHIM Meriem

State Engineer in Maintenance and Reliability of Industrial Systems
Master in Industrial Management

Theme:

Diagnosis of alternating current machine defects by time-frequency methods

Thesis defended on May 26, 2024 ahead the jury composed of:

N°	Full name	Degree	Institution	Quality
01	HADJADJ.A. Elyas	Prof.	Badji Mokhtar -Annaba University	President
02	MERABET Leila	MCA	Badji Mokhtar -Annaba University	Rapporteur
03	SAAD Salah	Prof.	Badji Mokhtar -Annaba University	Co-rapporteur
04	GHEMARI Zine	Prof.	M'silaUniversity	Examiner
05	CHEGHIB Hocine	Prof.	Badji Mokhtar -Annaba University	Examiner

Acknowledgement

This thesis is the result of work carried out at the Laboratoire des Systèmes Eléctromécaniques, Department of Electromechanics at Badji Mokhtar University - Annaba.

First of all, I would like to thank my supervisor and my thesis co-supervisor, Dr MERABET Leila and Pr. SAAD Salah, respectively, for their supervision and the wise advice they have given me throughout these years. They receive here the expression of my deep respect and with all my gratitude.

I would like to thank the president of the jury, Mr. HADJADJ.A. Elyas, professor at the University of Badji Mokhtar Annaba who kindly did me the honor of presiding over this jury. He finds here the expression of my deepest gratitude and respectful thanks.

I would also like to express my deepest thanks to the members of the jury, gentelmen: Mr. GHEMARI Zine, professor at the university of M'sila, and Mr. CHEGHIB Hocine, professor at the University of Badji Mokhtar Annaba for having done me the honor of judging this work as examiners.

I warmly thank all the members of my family and friends Basma and Nour El Houda for their encouragement, affection, and moral support.

Finally, I address my gratitude to all the teachers, who in some way contributed to this success even if they certainly do not remember me. May they find here the expression of my deep gratitude!

Dedication

In memory of my mother I lost in the beginning of the third year of my thesis

I wish you were here.

May God have your souls in his holy mercy

Not every letter can find the right words...

Not all words can express gratitude,

I promise to perpetuate your memory, as long as I'm in life.

No dedication can express my respect, my eternal love and my consideration for the sacrifices you have made for my instruction and my well-being.

To My father

I thank you for all the support and love you have shown me since my birth and I hope that your blessing always accompanies me.

May this modest work be the fulfillment of your many wishes, the fruit of your countless sacrifices, though I can never do enough for you.

May God, the Most High, grant you health and happiness and so that I will never disappoint you.

To my sister

I thank you for your help, encouragement, moral support and love.

May God bless you in your life.

Abstract

Powering production lines by means of asynchronous motors remains the most economical, robust and safest way for long periods of time. The durability of asynchronous motors is the major concern of maintenance technicians, which often requires diagnostic and maintenance actions.

This work is a contribution to the diagnosis of mechanical defects that can occur on asynchronous motors using vibration analysis. The work is divided into two experimental parts. In the first part, a whole experimental setup linked to accelerometers was set up to validate the bearing defects and build a database of vibration signals. In the second part, the same experimental setup was used but this time in conjunction with different mechanical defects.

The methods used for fault diagnosis and classification are: Wavelet Packet Decomposition (WPD) based on time-frequency methods, energy and L-kurtosis calculated from wavelet packet decomposition and perceptron multilayer based on artificial neural networks. The Multilayer Perceptron is involved to identify the type of defect in order to be able to establish a program of preventive or curative maintenance actions as soon as possible.

Keywords: Asynchronous motors; Diagnostic; Accelerometers; Wavelet packet decomposition; Time-frequency; Multilayer Perceptron; Artificial Neural Network; Energy; L-kurtosis.

مـــلـــخص

يظل تزويد خطوط الإنتاج بالطاقة عن طريق المحركات غير المتزامنة الطريقة الأكثر اقتصادا وقوة وأمانًا لفترات طويلة من الزمن. غالبًا ما تتطلب متانة المحركات غير المتزامنة ، الشاغل الرئيسي لفنيي الصيانة ، إجراءات التشخيص والصيانة.

هذا العمل هو مساهمة في تشخيص الأعطال الميكانيكية التي يمكن أن تحدث في المحركات غير المتزامنة باستخدام طريقة تحليل الاهتزاز. ينقسم العمل إلى جزأين تجريبيين. في الجزء الأول ، تم إعداد إعداد تجريبي كامل مرتبط بمقاييس التسارع لإنشاء عيوب المحامل وبناء قاعدة بيانات لإشارات الاهتزاز. في الجزء الثاني ، تم استخدام نفس الإعداد التجريبي ولكن هذه المرة بالاقتران مع مختلف العيوب الميكانيكية.

الطرق المستخدمة لتشخيص الأخطاء وتصنيفها هي: تحلل الموجات على أساس طرق التردد الزمني، والطاقة و عامل التسطيح L المحسوب من تحلل الموجات ، الشبكة العصبية الإدراكية متعددة الطبقات. تمّ إشراك نظام الإدراك متعدد الطبقات لتحديد نوع العيب من أجل التمكن من إنشاء برنامج إجراءات الصيانة الوقائية أو العلاجية في أسرع وقت ممكن.

الكلمات الرئيسية: محركات غير متزامنة؛ التشخيص؛ أجهزة قياس التسارع؛ التحلل في حزم الموجات؛ تردد الوقت متعدد الطبقات المستقبلات؛ شبكة أعصاب صناعية؛ طاقة؛ عامل التسطيح L.

Résumé

L'alimentation des chaines de production aux moyens de moteurs asynchrones reste le moyen le plus économique, robuste et le plus sûr pour de longues durées. La durabilité des moteurs asynchrones, le souci majeur des mainteniciens, exige souvent des actions de diagnostic et de maintenance.

Le présent travail est une contribution au diagnostic des défauts mécaniques qui peuvent survenir sur les moteurs asynchrones en utilisant l'analyse vibratoire. Le travail est scindé en deux parties expérimentales. En première partie, tout un montage expérimental lié à des accéléromètres été mis en place pour valider les défauts des roulements et construire une base de données des signaux vibratoires. En deuxième partie le même montage expérimental été utilisé mais cette fois ci en liaison avec différents types des défauts mécaniques.

Les méthodes exploitées pour le diagnostic et la classification des défauts sont: la décomposition en paquets d'ondelettes basé sur les méthodes temps-fréquence, l'énergie et le L-kurtosis calculé à partir de la décomposition en paquets d'ondelettes et le perceptron multicouches basé sur les réseaux de neurones artificiels. Le perceptron multicouches a été impliqué pour identifier le type de défaut afin de pouvoir établir un programme d'actions de maintenance préventive ou curative dans les meilleurs délais.

Mots clés: Moteurs asynchrones; Diagnostic; Accéléromètres; Décomposition en paquets d'ondelettes; Temps-fréquence; Perceptron multicouches; Réseau de neurone artificiel; Energie; L-kurtosis.

Scientific contributions

Research Paper

- M. Behim, L. Merabetand S. Saad, « Time - frequency method and artificial neural network classifier for induction motor drive system defects classification », Diagnostyka, p. 1‑11, janv. 2024, doi: 10.29354/diag/181192.

- Behim, M., Merabet, L. & Saad, S. Neural Network and L-kurtosis for Diagnosing Rolling Element Bearing Faults. J. Electr. Eng. Technol. (2024). https://doi.org/10.1007/s42835-023-01719-1.

International Conferences

- M. Behim, L. Merabet and S. Saad «Comparative study of time-frequency resolution: Application on broken rotor bars of an induction motor», International Conference on Innovative Applied Energy (Smart Exhibition) (DZENERGY), Hassi Messaoud, Ouargla, Algeria, 2021.

- M. Behim, L. Merabet and S. Saad, "Diagnosis of Supply Voltage Imbalance Using WPD Energy Enhanced by Current Space Vector (CSV)",2022 19th International Multi-Conference on Systems, Signals & Devices (SSD), Sétif, Algeria, 2022, pp. 242-245, doi: 10.1109/SSD54932.2022.9955936.

- M. Behim, L. Merabet and S. Saad, "L-kurtosis for mechanical load unbalance fault diagnosis" 1st International Conference on Trends in Advanced Research (ICTAR), Konya, Turkey, 2023.

- M. Behim, L. Merabet, S. Saad and B. Benbouya, "PMSM Short-Circuit Failure Detection Using Simulated Electric Data" 3rd International Conference on Innovative Academic Studies (ICIAS), Konya, Turkey, 2023.

National Conference

- M. Behim, L. Merabet and S. Saad «Detection and Classification of Induction Motor Faults Using DWPD and Artificial Neural Network: Case of Supply Voltage Unbalance and Broken Rotor Bars», 1st National Conference on Applied Science and Advanced Materials, Skikda, Algeria, 2021.

Contents

Chapter III: Diagnosis of bearing defects by vibration analysis

Chapter IV: Diagnosis of mechanical defects by vibration analysis

List of figures

Chapter I: Bibliographic review

Chapter II: Development of time-frequency methods and artificial neural networks

Chapter III: Diagnosis of mechanical defects by vibration analysis

Chapter IV: Diagnosis of mechanical faults by analysis of stator currents

List of tables

Chapter I: Bibliographic review

Chapter II: Development of time-frequency methods and artificial neural networks

Chapter III: Diagnosis of mechanical defects by vibration analysis

Chapter IV: Diagnosis of mechanical faults by analysis of stator currents

Glossary

Acronyms	
ACM	Alternating current machines
ADALINE	Adabtive linear neural network
ANFIS	Adaptive neuro-fuzzy inference system
ANN	Artificial neural network
ASM	Asynchronous machine
BBC	Broken bearing cage
CatGANs	Categorical generative adversarial networks
CNN	Convolutional neural network
CSV	Current space vector analysis
CWT	Continuous wavelet transform
CWScalogram	Continuous wavelet transform scalogram
db6	Daubechies 6
DCM	Direct current machines
DWPT	Discrete wavelet Packet transform
DWT	Discrete wavelet transform
EWT	Empirical wavelet transform
FFT	Fast Fourier transform
HS	Healthy state
IL	Improper lubrication
IM	Induction motor
KLD	Kullback-leibler divergence
LL	Lack of lubrication
LLBC	lack of lubrication+ broken cage
LMD	Local mean decomposition
LU	Load unbalance
MLP-NN	Multi layer perceptron neural network
MRA	Multi resolution analysis
MSE	Mean square error
MWC-FK	Morlet wavelet coefficients and fast kurtogram
MWR-DRN	Multiple wavelet regularized deep residual network
PCA	Principal Components Analysis
PM	Parallel misalignment
PNN	Probabilistic neural network
PR	Pattern Recognitions
QMF	Quadrature mirror filter
RBF	Radial basis functions
RMS	Root mean square
SELU	Scaled exponential linear units
SES	Squared envelope spectrum
SM	Synchronous machine
SPWVD	Smoothed pseudo Wigner Ville distribution
STFT	Short-term Fourier transform
SVM	Support vector machine
TF-AI	Time-Frequency and Artificial Intelligence

Acronyms	
TFR	Time-frequency representation
VMD	Variational mode decomposition
WBF	Wavelet basis function
WNN	Wavelet neural network
WPD	Wavelet packet decomposition
WPT	Wavelet packet transform
WPT-MWSVD	Wavelet packet transform- multi-weight singular value decomposition
WT	Wavelet transform
WVD	Wigner Ville distribution

Notations		
a	Hz	Dilatation
b	s	Translation
b_i	/	Bias
B	/	Resolution
B_D	mm	Ball diameter
C_D	mm	Pitch circle diameter
d	mm	Diameter of the rolling element
D	mm	Diameter of the pitch circle of the bearing
E_{rr}	/	Quadratic error
E_d	/	Energy density
E_j^n	/	Energy at level *j* node *n*
f	Hz	frequency
fa	/	Activation function
f_b	Hz	Ball defect frequency
f_{brb}	Hz	Broken rotor bar frequency
f_e	Hz	Power frequency
f_{ect}	Hz	Excentricity defect frequency
f_i	Hz	Inner race defect frequency
f_{max}	Hz	Maximum frequency
f_o	Hz	Outer race defect frequency
f_p	Hz	Pole passing frequency
f_r	Hz	Frequency of rotation
f_s	Hz	Sampling frequency
f_{su}	Hz	Supply frequency
f_{st}	Hz	Stator winding defect frequency
f_t	Hz	Train defect frequency
$h(t)$	/	Window function
LK_j^n	/	L-kurtosis at level *j* node *n*
Mu	/	The minimum change threshold of the error function between training iterations
N	/	Number of samples
N_c	/	Number of correct classification
N_t	/	Number of total tests
p	/	Number of poles
s	/	Slip
$s(t)$	/	Signal

Notations		
t	s	Time
T	s	Period
Ta	/	Target output
t_r	%	Performance rate
T_s	s	Sampling step
W_{in}	/	Weights
x_n	/	Input information
$\mathbf{x}_{\mathbf{k}}^{\mathbf{j+1}}$	/	Coefficients of wavelet packet decomposition
$\mathbf{Y}$	/	Calculated output
Z	/	Number of rollers/balls
α	radian	Bearing contact angle
σ	/	Standard deviation
τ	s	Translation in time
Ψ	/	Mother wavelet function
Ψ^*	/	Complex conjugate of Ψ

General introduction

Alternating current machines (ACMs) were the immense contribution of Nikola Tesla to science and technology which was noted around the years 1887-1888 in his patent and publication, of which he explained the principle of operation of his discovery[1], [2].

ACMs are divided into two categories. Synchronous machines (SM) whose rotational speed of the rotor is equal to the rotational speed of the rotating field, this is called synchronism speed; and asynchronous machines (ASM) whose rotor speed is slightly lower than the rotational speed of the rotating field; the relative speed between the rotor and the rotating field is called slip[3].

This type of machines is widely used for applications that does not need high precision; they are characterized by their power, robustness, ease of implementation and low cost[3].

Therefore, many diagnostic techniques are developed to identify the most critical defects occurring on ACMs, more precisely the asynchronous motors, called also induction motors (IMs),in order to prevent breakdowns, improve the operating time and minimize the shutdown cost. All faults that occur on IMs can be classified into several categories: stator and rotor defects; electrical, mechanical and environmental defects or internal and external defects. The IMs defects are expected, according to IEEE study results on induction motor faults[4], as follow: 42% of defects represents bearing damages and 28% is for stator winding damages where rotor related damages are of 8% , the rest of 22% includes other IM defects.

To diagnose these defects, a multitude of model based approaches and modeless approaches are developed. For model based approaches we can cite parametric estimation analysis, observer-based analysis and parity space analysis. The modeless approaches can be divided into static methods (Statistical test, Principal Components Analysis (PCA), Pattern Recognitions (PR), Bayesian Network and Hidden Markov Model); signal processing methods (Temporal analysis, Frequency analysis and Time-frequency analysis) and artificial intelligence approaches (Neural networks, Fuzzy logic, Neuro-Fuzzy logic and Support Vector Machine (SVM)). These methods are exploited, using several condition monitoring techniques such as vibration analysis techniques and motor current signature that are the most used in the literature; the air-gap torque that can be measured when the IM is operating[5]. The magnetic flux monitoring used to identify several stator and rotor defects by calculating magnetic flux density through it. The speed fluctuation monitoring technique, used to detect rotor defects during the operating time of the machine.

The surge testing technique which is mainly used to predict the failure of the insulation and the unbalance of the winding before the occurrence of a turn-turn short circuit using overvoltage testers; motor circuit, a non-invasive technique, that calculates the electrical and magnetic parameters, and tests the insulations in order to evaluate the state of the motor; gas analysis technique which is based on infrared absorption method that detect the state of electrical insulation using carbon monoxide produced from its degradation after a set of electrical reactions [4].Acoustic emission which is typically applied for composite material structurally modified under stress which create a rapid liberation of energy deformation, and so a generation of transient elastic wave [6-8]; temperature monitoring, a non-destructive technique, which coming widely used for the detection of IM defects[5], it is based on picking up the over-heat produced from several defects affecting the IM components[6] and partial discharge monitoring that can be performed as an on-line quality control test during normal operating conditions[9].

Although the variety of the proposed methods, the latest works are based on the signal processing methods by time-frequency methods as short time Fourier transform (STFT), Wigner Ville distribution (WVD) and wavelet transformer (WT). These techniques are associated to artificial intelligence techniques as Artificial Neural Network (ANN), Fuzzy Logic, Neuro-Fuzzy Logic etc., in order to classify and improving fault recognition.

It is for this reason that this thesis aims to address several types of IM defects, which are not fairly treated in previous researches through vibration analysis technique; using a novel methodology, that will be detailed in chapters 3 and 4. This methodology is based on the wavelet packet decomposition that represents the best time-frequency method due to its better resolution over the other time-frequency approaches and the MLP-NN as the easiest and most popular AI technique for its application, with an integration of novel combined features.

In order to conduct this study, the content of the present thesis is organized into four chapters: chapter 1 presents a bibliographic review related to the theme of the thesis. The theoretical background of the time-frequency methods and ANN approaches are introduced in chapter 2. chapter 3 and 4 are devoted to the experimental setup for data acquisition and the proposed method for bearings and IM mechanical fault diagnosis respectively. The analysis is carried out through the wavelet transform and the Multi-Layer Perceptron Neural Network using vibration analysis technique and confirm the efficiency of the proposed method. Finally, general conclusion and future trends are given.

Chapter I
Bibliographic review

I.1 Introduction

Rotating electrical machines are reversible electromechanical systems that transform electrical energy into mechanical energy (motor operation) and vice versa (generator operation) [3].

There are two main families of electrical machines: direct current machines (DCM) and alternating current machines (ACM).

ACMs themselves break down into two types: synchronous machines and asynchronous machines.

Asynchronous motors, which are part of asynchronous machines, are also known as induction motors (IM).

For decades, induction motors have enjoyed wide use in domestic and industrial fields because they are more robust, require less maintenance, and are more economical in terms of manufacturing and operating costs. Asynchronous motors do not have brushes like direct current motors, which significantly reduces wear and the need for maintenance. Additionally, they offer better energy efficiency and durability, making them ideal for industrial use where reliability and longevity are essential. For this reason, several works focus on the study of induction motors while developing methods for diagnosing their defects using different condition monitoring techniques (Table I. 1) for data acquisition enabling effective condition monitoring, extending machine life and minimizing unplanned downtime. Then appropriate maintenance actions are taken into account to restore the machine to its initial state. Where there are many types of maintenance can be resumed by Figure I. 1 [10].

Table I. 1 Comparisons of main condition monitoring techniques

Technique	Fundamental principles	advantages	Disadvantages
Vibration analysis	Measures vibration levels and frequencies to detect imbalances, misalignments, bearing defects, etc.	Effective for rotating equipment, detects a wide range of mechanical problems.	Requires specialist equipment and skills, results influenced by external noise.
Oil analysis	Analyzes lubricating oil properties and composition to identify wear particles, contaminants, and degradation.	Provides information on internal component wear, detects lubrication and contamination issues.	Requires regular sampling and laboratory analysis, results may be delayed.
Thermography	Uses infrared cameras to detect temperature variations on the surface of equipment, identifying hot spots indicative of problems such as electrical faults or poor lubrication.	Non-invasive, provides a visual representation of temperature distribution, useful for electrical and mechanical systems.	Limited to detection of surface temperature variations, requires interpretation by qualified personnel.
Electrical analysis	Analyzes electrical signals and power quality to identify electrical and mechanical faults in electrical motors and generators.	Non-invasive, can be performed online, detects a wide range of electrical and mechanical problems.	Requires specialized equipment and skills, complex interpretation of electrical signals.

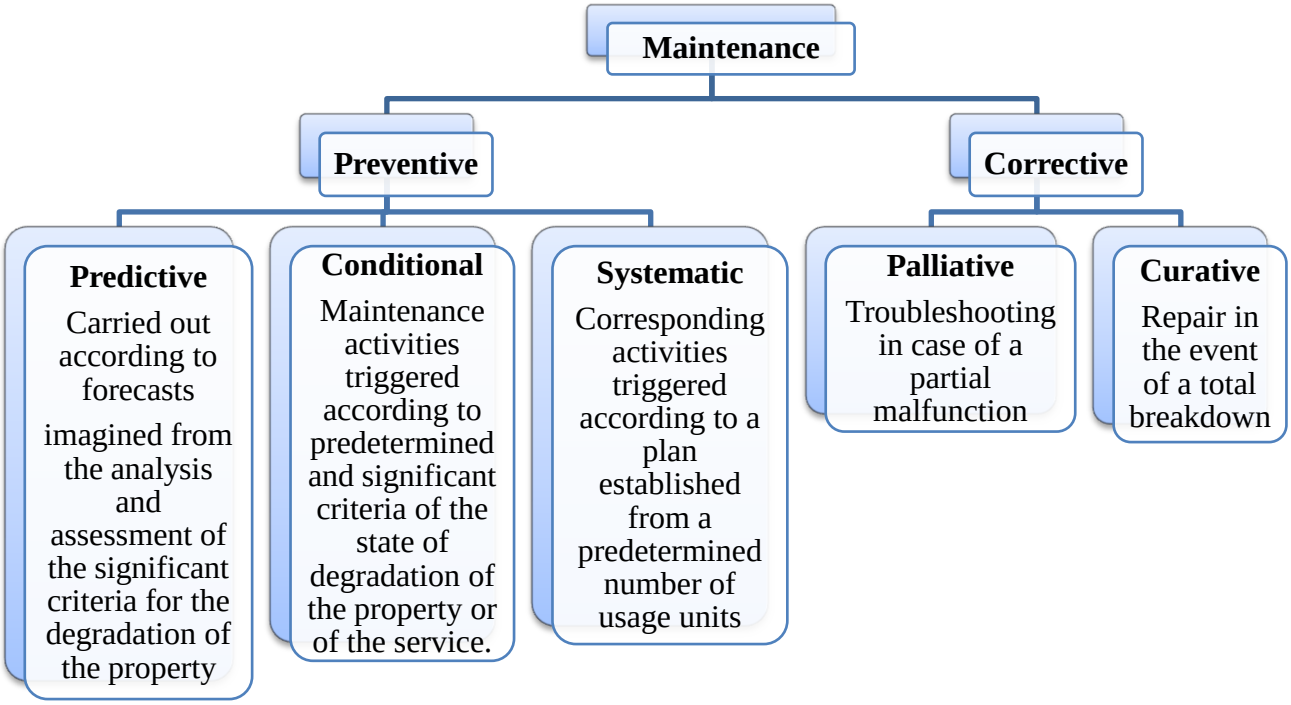

Figure I. 1 Maintenance types

I.2 Bibliographic review

In recent years, works are based on the processing of defective signals by time-frequency methods such as the short-time Fourier transform (STFT), the Wigner Ville distribution (WVD) and the wavelet transform (WT) using several diagnosis techniques.

Approaches based on signal processing simultaneously in time and frequency have aroused great interest.

Gaied and al.[11] applied the DWT (discrete wavelet transform) method on four types of signals: stator current, torque, flux and speed in order to diagnose the faults of the variable load short circuit.

In order to detect the absence of one of the supply current phases fault during motor operation, Haouem and al.[12] analyzed the stator current using all the methods: park vector, Fourier transform, mean square spectrum, Hilbert transform and the STFT (short-term Fourier transform).

Lahouasnia and al.[13] extended the WPT (wavelet packet transform) for detection unbalance defects on induction motors. They combine wavelet package transform WPT and CSV

(current space vector) analysis in order to improve efficiency to detect load unbalance fault with different weights that yield more explanatory energy levels.

Sonje and al.[14] carried out the discrete wavelet transform (DWT) on the Park's vector modulus of current signals to detect the turn to turn short-circuit fault in stator winding. They studied the best-fitting mother wavelet by testing various orthogonal wavelet functions on simulated signals and tested on experimental current signals under operating conditions like balanced, unbalanced supply voltages and load slip variation.

While Zhang and al.[15] combined Q-factor Gabor wavelets and CWT (continuous wavelet transform) to generate better time-frequency resolution. They applied this methodology to a set of vibration signals to diagnose bearing defects.

Belkacemi and Saad [16] gave an overview on a famous time-frequency type signal processing method, namely, DWT (discrete wavelet transform) method, for the detection of bearing lubrication defects. In particular, in this study, they described the simplicity and effectiveness of this method. They applied DWT to vibration signals from an induction motor in healthy and faulty states.

Huang and al.[17] give improvements to the EWT (empirical wavelet transform) method dedicated to bearing fault diagnosis through vibration analysis. This improvement aims to reduce the loss of information (characteristic fault frequency of bearings) due to the breakage of the bands, obtained as a result of the decompositions, by the optimization of the frequency band region on the basis of the set of parameters: mean and variance.

The study of Chen and Feng [18] was based on the processing of stator currents in the presence of planetary gear defects and an air gap eccentricity using adaptive iterative generalized demodulation technique based on Hilbert transform and Fourier transform.

Liu and al.[19] studied vibrational signals containing bearing defects, using mainly, the fast kurtogram to separate the optimal frequency band, and the time-frequency representation (TFR) of the envelope obtained by the adaptation of the Hilbert transform with the STFT for the filtered signal. Then, the instantaneous fault characteristic frequency is extracted from the filtered fast Fourier transform (FFT) based on an improved instantaneous frequency estimation algorithm.

Yu[20] used a method called the transient extraction transformation, with the goal of efficiently characterizing and extracting transient components in faulty signals.

This method is based on the short-time Fourier transform (STFT) and the spectral flattening parameter (kurtosis).

In order to refine the results of these time-frequency methods, several articles introduce the tools of artificial intelligence as classifiers of the various faults. For example, in the field of bearing fault diagnosis, Anbu and al. [21] used the combination DWT (discrete wavelet transform) and fuzzy logic (fuzzy c-means clustering) through scalar indicators (Average, variance, kurtosis, RMS, peak to peak, S-factor, C-factor, I-factor).

While, Djaballah and al.[22], first, dealt with different bearing faults by using several types of wavelet with different levels of decomposition, the two scalar indicators (energy and kurtosis) and the multilayer perceptron neural network for classification. As a result, they selected the mother wavelet, which gave better accuracy, namely db6 (Daubechies 6).

Quinde and al.[23] considered the problem of the presence of cross-terms when applying the WVD (Wigner Ville Distribution) method on multi-component signals which can give misleading interpretations of the defects. For this, they integrated the Local Mean Decomposition (LMD) approach in their methodology, to obtain a more reliable diagnosis based on vibrational signals. Moreover, they selected the optimal frequency band with the most relevant defect information using the Kullback-Leibler Divergence (KLD).Due to this, they could identify defects during classification by feed-forward neural networks.

Singh and Shaik [24] detected, classified and located bearing faults through stator voltage and current signals. In this study, they proceeded a set of approaches; they applied FFT (Fast Fourier Transform) and Stockwell transform to extract a number of features in time and frequency domain and SVM (Support Vector Machine) for classification.

To improve the performance of the SVM (support vector machine) classifier, Tajeddini and al.[25] presented a new methodology based on the two approaches, Dempster-Shafer theory and WPT (wavelet packet transformation). In this research, they identified bearing defects whose data is acquired by a double sensor, one for vibration measurements and the other for current measurements. They used for this, wavelet packet transformation for each sensor as an

efficient pre-processing method for signal denoising, and Dempster-Shafer theory to merge the SVM classifier decision.

Attoui and al.[26] proposed an algorithm, for bearing fault diagnosis, that includes four key steps: data acquisition, feature generation, feature selection, and defect classification. For this, they employed, while basing on the envelope model, the following methods: the DWPT (discrete wavelet packet transform), the FFT (fast Fourier transform) and the ANFIS (adaptive neuro-fuzzy inference system).

The methodology of Niloofar Gharesi and al.[27] proposed for the diagnosis of the same type of defect is based on non-recursive variational mode decomposition (VMD) for feature extraction, and WNN (Wavelet Neural Network) for classification, through a set of statistical indicators .

Pavan Agrawal et Jayaswal [28] made a comparative study between artificial neural network (ANN) and support vector machine (SVM) using continuous wavelet transforms (Morlet wavelets) and energy entropy approaches for the diagnosis and classification of bearing faults.

Tao and al.[29] have proposed an algorithm named St-GatGAN intended for bearing fault diagnosis by vibration analysis. For this, they first introduced STFT to transform the raw one-dimensional (1D) vibration of signals into 2D time-frequency maps to serve as input to CatGANs (Categorical Generative Adversarial Networks). Then, it obtains a model CatGAN through an adversarial training process to generate fake samples with a distribution similar to the maps extracted by STFT and cluster the input samples into certain categories.

In order to diagnose bearing faults through vibration analysis, Zhang and al.[30] presented a simple methodology that can improve the results of the CNN (convolution neural network) classifier. They applied STFT (Short Term Fourier Transform) to get an input image, then Exponential Linear Scale Unit (SELU) function is introduced to avoid excessive dead nodes during the learning process, and hierarchical regularization to get better results from neural network training.

Zhao and al.[31] attempted to improve diagnostic accuracy when training data is insufficient by developing a multiple wavelet regularized deep residual network (MWR-DRN) model that uses a wavelet basis function (WBF). This method is tested by vibration signals in the healthy state and in the presence of different types of bearing and gear defects.

Table I.2 summarizes the researches cited in the present chapter.

I.3 Conclusion

TF-AI (Time-Frequency and Artificial Intelligence) approaches, for efficient diagnosis of IMs, have received considerable attention from various studies, while introducing a set of scalar indicators.

However, there are still many difficulties in implementing TF-AI methods for real diagnosis due to the specific features (e.g., multi-variety, non-linearity, non-stationarity, etc.). Thus, to bridge the moderately large gap between theoretical approaches and implementations, it is necessary to consider new hybrid approaches as well as to design more elaborate TF-AI models using various combined techniques (time-frequency, scalar indicators and artificial intelligence).

Table I.2 Bibliographic review

Ref	Fault types	Exploited techniques	Proposed methods	Results
[10]	Short circuit	Stator current, torque, flux and speed	DWT	Fast detection of defects
[11]	Absence of one of the supply current phases	Stator current	Park vector; Fourier transform; mean square spectrum; Hilbert transform and the STFT	The operator is able to observe and make quick, dependable judgments on the engine's performance thanks to the realistic results that demonstrate the efficacy of the suggested methodology
[12]	Load unbalance fault	Stator current signals	WPT; CSV; energy	The suggested method's capacity to distinguish between a healthy state and various degrees of load unbalance defects
[13]	Turn to turn short-circuit fault	Stator current signals	Park’s vector modulus; DWT	DWT demonstrated its sensitivity and robustness for fault detection; and the fault severity factor enhanced the assessment of the IM fault severity .

Table I.1 (continue)

Ref	Fault types	Exploited techniques	Proposed methods	Results
[14]	Bearing defects	Vibration	Q-factor Gabor wavelets; CWT	The resolution of the time-frequency method was improved in extracting information and identifying the faults
[15]	Bearing lubrication defects	Vibration	DWT	The DWT decomposition approach was found to be effective in differentiating between a healthy bearing and an improperly lubricated bearing at medium speeds.
[16]	Bearing defects	Vibration	EWT	In comparison to using simply scale space approaches, an enhanced EWT method was presented that can extract the fault characteristic frequency more easily and effectively while avoiding over segmentation and redundancy.
[17]	Planetary gear defects; air gap eccentricity	Stator currents	Adaptive iterative generalized demodulation	The modification in Adaptive iterative generalized demodulation procedure prove its ability to be extended to deal with MCSA field in order to identify and display weak time-varying fault signals on the time-frequency plane
[18]	Bearing defects	Vibration	Fast kurtogram; Hilbert transform; STFT; FFT	The suggested method's capacity to identify and locate the bearing failure without requiring a rotational frequency measurement as a reference.

Table I.1 (continue)

Ref	Fault types	Exploited techniques	Proposed methods	Results
[19]	Bearing defects	Vibration	Transient extraction transformation	The suggested approach performs the best when enhancing energy concentration and breaking down transient components with the largest kurtosis; with the same computing complexity of the STFT
[20]	Bearing defects	Vibration	DWT; fuzzy c-means clustering; scalar indicators	High classification accuracy of 100%
[21]	Bearing defects	Vibration	WPD; ANN; Energy; Kurtosis	Maximum classification accuracy of 99.47 %
[22]	Bearing defects	Vibration	LMD; KLD feed-forward neural networks	Average classification accuracy of 98.5 %
[23]	Bearing defects	stator voltage; current signals	FFT; Stockwell; SVM	Average classification accuracy of 95 %
[24]	Bearing defects	Vibration; current measurements	Dempster-Shafer theory; WPT; SVM	A better Classification accuracy was obtained when dealing with SVM classifier
[25]	Bearing defects	Vibration	DWPT; FFT; ANFIS	High classification accuracy of 99.83%
[26]	Bearing defects	Vibration	non-recursive WNN; statistical indicators	High classification accuracy of 99.48%
[27]	Bearing defects	Vibration	ANN; SVM; Morlet wavelets; energy entropy	High classification accuracy of 100%
[28]	Bearing defects	Vibration	St-GatGAN	Average classification accuracy of 91.89%
[29]	Bearing defects	Vibration	STFT; SELU; CNN	Average classification accuracy of 97.81%
[30]	Bearing and gear defects	Vibration	MWR-DRN	Classification accuracy of 96.67%

Chapter II
Development of time-frequency methods and artificial neural networks

II.1 Introduction

In recent years, as shown in the first chapter, research has been based on the combination of time-frequency type signal processing methods, also called time-scale representation, and artificial intelligence tools. We have directed our research towards the introduction of artificial neural networks through the intermediary of the scalar indicators which will be presented in this chapter.

This chapter will therefore be devoted to the study of the main time-frequency transformations as well as the artificial neural networks that we have detailed in order to choose the most suitable combination for our research; but before that, we chose to make a general overview on the signals.

II.2 General information on signals

II.2.1. Signal definition

A signal is the physical representation of the information, it transmits from its source to a recipient. It represents an information carrier[32].

In other words, it is the physical manifestation of a measurable quantity (vibration, current, voltage, pressure..etc.).

II.2.2. Signals classification

Different ways of classifying the models of the signals can be envisaged, of which we cite[32]:

- Phenomological classification, we emphasize the signal's type of evolution, its predetermined character and its random behavior,
- Morphological classification according to continuity or discretization of signals,
- Energy classification, spectral classification and dimensional classification.

By following the first so-called phenomological classification, we can break down the types of signals as follows:

- Deterministic signals, whose signals can be predefined by a mathematical model (a well-determined mathematical function). For this type of signals we find:

  - Periodic signals which include sinusoidal, composite periodic and pseudo-random signals.
  - Non-periodic signals, that are quasi-periodic signals and transient signals.
- Random signals, whose temporal behavior is unpredictable that can be stationary type, where the frequency content unchanged in time, or non-stationary type where the frequency content changes in time.

II.2.3. Signal sampling

Sampling is the regular or irregular sampling of point values using a digital electronic system, namely the computer, from analog signals [32].

Generally, the type of accredited sampling is regular (periodic) sampling with a constant sampling interval T_s.

In the case of low-pass spectrum signals with bounded support, according to Shannon's theorem, the regular interval T_s must be less than or equal to $1/(2f_{max})$, to ensure the reconstruction of the analog signal from the samples, .i.e. avoid the loss of information when converting analog signals to digital signals by the sampling operation [32].

II.2.4. Signals resolution

The resolution depends on the finite observation time T of the signal. This duration is equal to the product of the number of samples N and the sampling step T_s [32].

$$\mathrm{T} = \mathrm{N} * \mathrm{T_s} \tag{II.1}$$

Hence, the resolution B is represented by:

$$B = \frac{1}{T} = \frac{1}{N*T_s} = \frac{f_s}{N} \tag{II.2}$$

II.2.5. Signal filtering

The purpose of filtering is to alter the frequency spectrum of signals to eliminate or enhance certain frequency ranges or bands.

The filters are linear systems, characterized by linear differential equations with constant coefficients. They can be studied by their Laplace transmittance, in terms of their temporal

behavior (impulse response, step response), or by their harmonic transfer function, in terms of their frequency behavior.

The main types of filters are: low-pass, high-pass, band-pass, band-stop (or band-rejector). There are also other filters which do not modify the gain but only the phase, called pure phase shifters [33].

II.3 Time-frequency methods

II.3.1. Short time Fourier transform

- **Fourier transform and its limitation**

The Fourier Transform decompose the signal $f(t)$ in infinite number of sine/ cosine waves witch called harmonics [34]. The Fourier transform for continuous time signals can be expressed as:

$$F(f) = \int_{-\infty}^{+\infty} f(t) e^{-2\pi \mathrm{ft}}\, dt \tag{II.3}$$

And for discrete time signals we use this equation:

$$F(f) = \sum_{-\infty}^{+\infty} f(n) e^{-2\pi f n} \tag{II.4}$$

There is no means of identifying exactly where an event occurs. In magnitude representation versus frequency, the time is messing. As a result does not cope well discontinuous bursts of signals in time domain. The Fourier transform cannot precise at what time the frequency components occur [34].

- **Short time Fourier transform**

The short-time Fourier transform (STFT), is a linear transform based on the development of the standard Fourier transform technique, proposed by Denis Gabor in 1946 [35]. This technique, called signal windowing, uses a fixed-width sliding window and analyzes only a small portion of a signal at a time assuming the signal segment is stationary. The downside of STFT is that the width of the window is unchanged. On the other hand, it is faced on the resolution dilemma: if we choose a narrow window, we obtain a good temporal resolution and a poor frequency resolution, and vice versa, if we choose a wide window, we obtain poor time resolution and good frequency resolution as shown in Figure II.1.

Therefore, this approach is not suitable for characterizing the local time-frequency characteristic of non-stationary signals [36]. It is obvious that many STFTs with different frequency resolutions should be tried and compared to improve the detection of transients of unknown shapes [37].

STFT allows useful signal information to be monitored under changing speed conditions [38]. It can be represented by [39]:

$$STFT(\tau, f) = \int_{-\infty}^{+\infty} s(t)h^*(t-\tau)e^{-j2\pi ft}\,dt \qquad \text{(II.5)}$$

where *s(t)*is the signal and *h*(t)* is the complex of the window function whose position has been translated in time by τ.

And, the corresponding energy density called the spectrogram is defined by squared modulus of the short-term Fourier transform formula, such as [39]:

$$E_d = |STFT(\tau, f)|^2 \qquad \text{(II.6)}$$

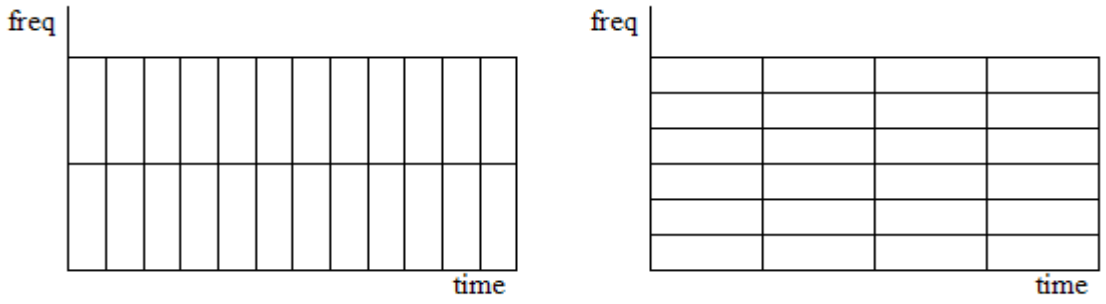

Figure II.1 STFT resolution problem

II.3.2. Wigner Ville Distribution

Wigner Ville Distribution (WVD) , is a quadratic nonlinear time-frequency distribution, defined as the Fourier transform of the local autocorrelation function of the signal *x(t)* [23], [36], expressed by:

$$WVDx(t,f) = \int_{-\infty}^{+\infty} x\left(t-\frac{\tau}{2}\right)x^*\left(t+\frac{\tau}{2}\right)e^{-j2\pi f\tau}\,d\tau \qquad \text{(II.7)}$$

This approach uses the interference of the cross terms by calculating the instantaneous autocorrelation function; at the same time achieves the best energy concentration for linearly frequency modulated signals (or chirps) [36]. This is why an improved version of WVD

called Smoothed Pseudo Wigner Ville Distribution (SPWVD) was invented in order to remove cross terms [23]. SPWVD is defined as:

$$\mathrm{SPWVDx}(t,f)=\int_{-\infty}^{+\infty} g(t)H(f)x\left(t-\frac{\tau}{2}\right)x^{*}(t+\frac{\tau}{2})\,e^{-j2\pi f\tau}d\tau \qquad \text{(II.8)}$$

II.3.3. Wavelet transform

II.3.3.1. Historic

The wavelet transform is a powerful tool in area of signal processing. The wavelet transform also known as multi-resolution analysis. First wavelet, known as the Haar wavelet, is introduced by Alfred Haar; it is defined as a function composed of a short negative pulse followed by a short positive pulse.

Later, Jean Morlet and Alex Grossmann introduced the term wavelet to the mathematical language in 1984. Yves Meyer collected all the previous results, calculated 16 of them, then defined orthogonal wavelets. Then, Stéphane Mallat established a link between wavelet analysis and multi-resolution analysis. Finally, in 1987, Ingrid Daubechies developed an orthogonal wavelet, easy to implement, called Daubechies wavelet [40].

II.3.3.2. Wavelet family

A wavelet is a waveform of effectively limited duration that has an average value of zero.

It is a mathematical object used for signal processing. They allow particular to decompose a signal in a frequency domain whose precision varies depending on the frequency band considered.

A wavelet has several proprieties like:

Compact support: Most wavelets are compactly supported in the time domain, which means that they are of finite duration and are distinguished by their rapid attenuation. A compact support allows reduced computational complexity, better resolution in the time domain but gives poor frequency resolution. As example, we can cite Daubechies wavelets, Symlets, Coiflets, etc. By duality, narrow band wavelets are compactly supported wavelets in the domain frequency but not in the time domain. Meyer wavelets are one example [34].

Regularity: The regularity of a wavelet is the property making it possible to locate the singularities in a signal. It can be noted that there is a link between regularity and the zero moments. As much as we have zero moments, the signal is regular [34].

Symmetry: like the number of zero moments, the symmetry of the wavelet conditions the regularity of it over an interval [34].

Orthogonality: The orthogonality of a wavelet is the property allowing eliminating information redundancy [34].

There are several mother wavelets used for calculating the wavelet transform analyzed signals. Each of them has a defined domain of application in the form of signal studied.

Table II.1 and Figure II.2 contain the most common families:

Table II.1 Types of wavelet family

Wavelet family name	**Abbreviation**
Haar wavelet	Haar
Daubechies wavelet	Db
Symlets wavelet	Sym
Coiflets wavelet	Coif
Biorthogonales wavelet	Bior
Meyer wavelet	Meyr
Gaussiennes wavelet	Gaus
Gaussiennes complexes wavelet	Cgaus
Mexicain wavelet	Mexh
Morlet wavelet	Morl
Morlet complexes wavelet	Cmor
Shannon complexes wavelet	Shan

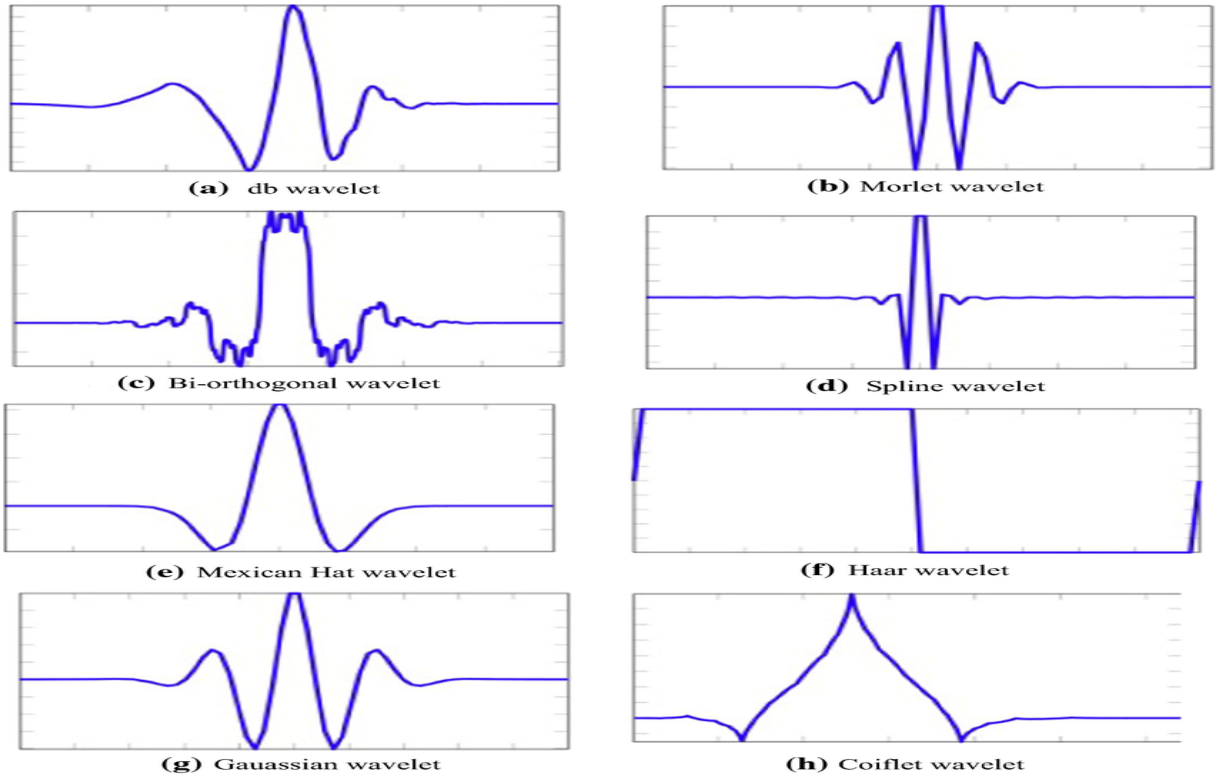

Figure II.2 Examples of wavelet families[41]

Wavelet families can be characterized by four properties main existence of associated filters, orthogonality or biorthogonality, support compact or non-compact, real or complex wavelets. Table II.2 summarizes these various properties.

Table II.2 Wavelet family proprieties

Wavelet with filter			**Wavelets without filters**	
with compact support		**with non-compact support**	**Real**	**Complex**
Orthogonal	**Biorthogonal**	**Orthogonal**		
Db, haar, sym, coif	Bior	Meyr	Gaus, mexh, morl	Cgau, shan, Cmor

II.3.3.3. Principle of wavelet transform

Unlike the short-term Fourier transform method, the wavelet transform uses an automatically adjustable width window for low and high frequencies, with a resolution adaptive to the size of the object or the analyzed detail, which facilitates localization defects. It uses windows with narrow time widths for high frequency components and windows with long time widths for low frequency components (Figure II.3). Hence, each frequency of the component receives the same treatment without reinterpreting the result, which provides more support for

the wavelet transform to analyze signals with local transient components. Time-frequency positioning means more energy wavelet coefficients are located, which is useful for feature extraction [40]. This technique decomposes the signal based on particular functions called wavelets which have the property of being able to be well localized in time or in frequency due to its basic elements, generated by translation *b* and dilation *a* from a mother wavelet function , as shown in the following expression:

$$\Psi_{a,b}(t) = \frac{1}{\sqrt{a}}\Psi\left(\frac{t-b}{a}\right) \qquad a, b \in R \tag{II.9}$$

a, b are called dilatation (scale) and translation (position) parameters respectively.

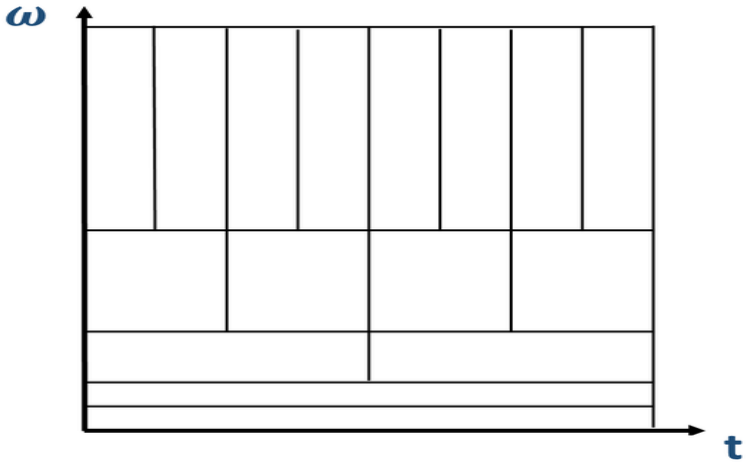

Figure II.3 Resolution of wavelet transform

II.3.3.4. Types of wavelet transform

There are many types of wavelet transforms, such as continuous wavelet transform (CWT); Discrete wavelet transform (DWT) and Wavelet packet decomposition (WPD).

- **Continuous wavelet transform**

When the structural parameters (the translation *b* and the dilation *a*) used can take any value of the set of real numbers *R* (the dilation *a* must be positive) we say that this wavelet transform is continuous[40].

The continuous wavelet transform is similar to the short-term Fourier transform (STFT), except that the sliding window used for the analysis changes over time [42].

The continuous wavelet transform of a function *x(t)* is defined as the inner product [42]:

$$CWT(a,b) = \langle x, \Psi_{a,b} \rangle \quad \text{(II.10)}$$

It means:

$$CWT(\mathrm{a},\mathrm{b}) = \frac{1}{\sqrt{\mathrm{a}}} \int_{-\infty}^{+\infty} x(\mathrm{t}) \Psi^{*} \left(\frac{\mathrm{t}-\mathrm{b}}{\mathrm{a}} \right) \mathrm{dt} \quad \text{(II.11)}$$

with:

Ψ^{*} is the complex conjugate of the mother wavelet Ψ.

b is the time location parameter.

a is the frequency localization parameter.

$\sqrt{a}$ ensures the same energy for the dilated wavelet.

- **Discrete wavelet transform**

The discrete wavelet transform (DWT) is a discretization of the continuous wavelet transform (CWT) by fixing 2^{m} and $\mathrm{n}2^{\mathrm{m}}$ instead of *a* and *b* respectively, with *m* and *n* being integers [43], and so :

$$DWT(\mathrm{m},\mathrm{n}) = \frac{1}{\sqrt{2^{\mathrm{m}}}} \int_{-\infty}^{+\infty} x(\mathrm{t}) \Psi^{*} \left(\frac{\mathrm{t}-\mathrm{n}}{2^{\mathrm{m}}} \right) \mathrm{dt} \quad \text{(II.12)}$$

The families of common discrete wavelet transforms are: discrete Coiflet wavelet, Cohen Daubechies wavelet, binomial-quadrature mirror filter (QMF), Daubechies wavelet, Haar wavelet, Mathieu wavelet, Legendre wavelet [11].

The discrete wavelet transform (DWT), has a major drawback, the inability to decompose high frequency sub-bands, i.e., the wavelet transform only iterates over the scaling coefficients (approximation) (Figure II.4).

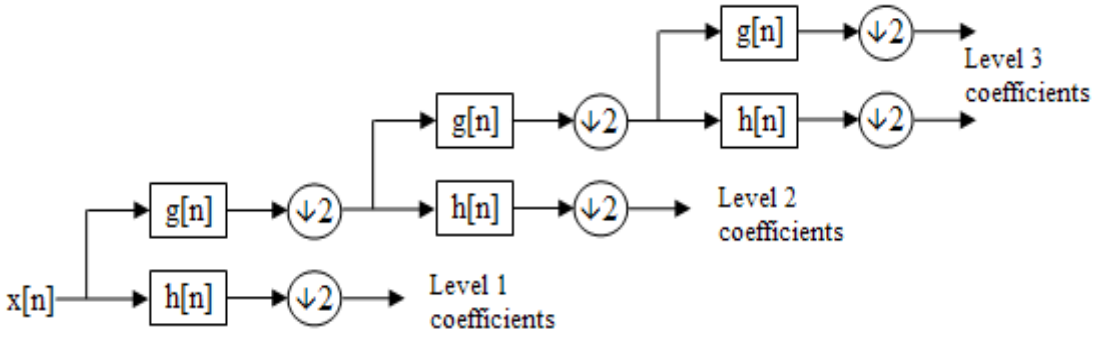

Figure II.4 DWT Tree

- **Wavelet packet decomposition**

The wavelet packet decomposition (WPD), proposed by Coifman and Wickerhauser, unlike the discrete and continuous wavelet transform, generates at each level an approximation coefficient containing low frequency information, and a detail coefficient containing high information. frequencies of the original signal without data loss or redundancy. The operation can be repeated at several levels and leads to the creation of the tree structure represented on the Figure II.5 [13], [44].

Coefficients of wavelet packet decomposition (X_k^{j+1})are defined as[45]:

$$\begin{cases} X_{2p}^{j+1}[n] = \sum_m HP[m-2n]X_p^j[m] \\ X_{2p+1}^{j+1}[n] = \sum_m LP[m-2n]X_p^j[m] \end{cases} \quad \text{(II.13)}$$

p=0,1,2...,2^{j-1} : the numbered nodes at level *j*.

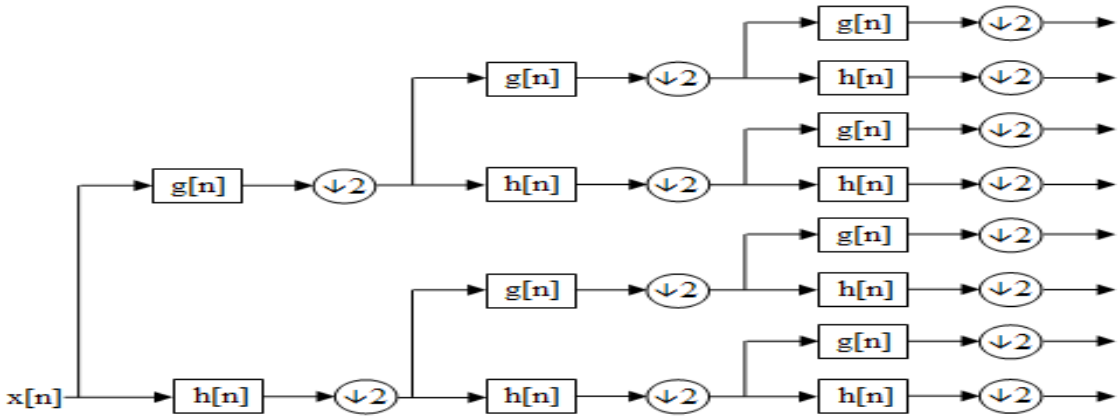

Figure II.5 WPD tree

The level of wavelet decomposition, must be well chosen so that it includes the harmonics around the fundamental frequency of the signal [42], it is calculated by the relation:

$$N = int\left(\frac{\log\left(f_s/f_e\right)}{\log(2)}\right) + 2 \quad \text{(II.14)}$$

f_s, sampling frequency and f_e, power frequency.

II.4 Artificial neural networks

II.4.1. History

The artificial neural network is a mathematical model whose design is inspired by the function of biological neurons [46].

An early wave of interest in neural networks (also known as connectionist models or distributed parallel processing) emerged after the introduction of neurons by McCulloch and Pitts in 1943[47].

II.4.2. Usefulness

Neural networks (NN) have been widely applied to real-world problems in security, science, engineering, medical science, agriculture, finance, banking, education, energy, management, manufacturing, etc. as a method of optimization, intrusion detection and for data and images classification [48].

II.4.3. Artificial Neuron

Artificial neuron is a fundamental building block of artificial neural networks, which are used in machine learning and deep learning algorithms for pattern recognition, classification, and regression task. The artificial neural network is composed of an input layer, one or more hidden layers and an output layer [49]. The resulting data from each layer represents inputs for the layer that follows it, where, these data are weighted by weights (w_i) subject to learning errors [50] according to rules and algorithms from which we cite: gradient descent algorithm, Heb's law, Delta's rule, Window-Hoff's algorithm, Gross-Berg's law...etc.

An artificial neuron is a mathematical model inspired by the biological neurons in the human brain. The model of the artificial neuron can be represented by the diagram of the Figure II.6 [51].

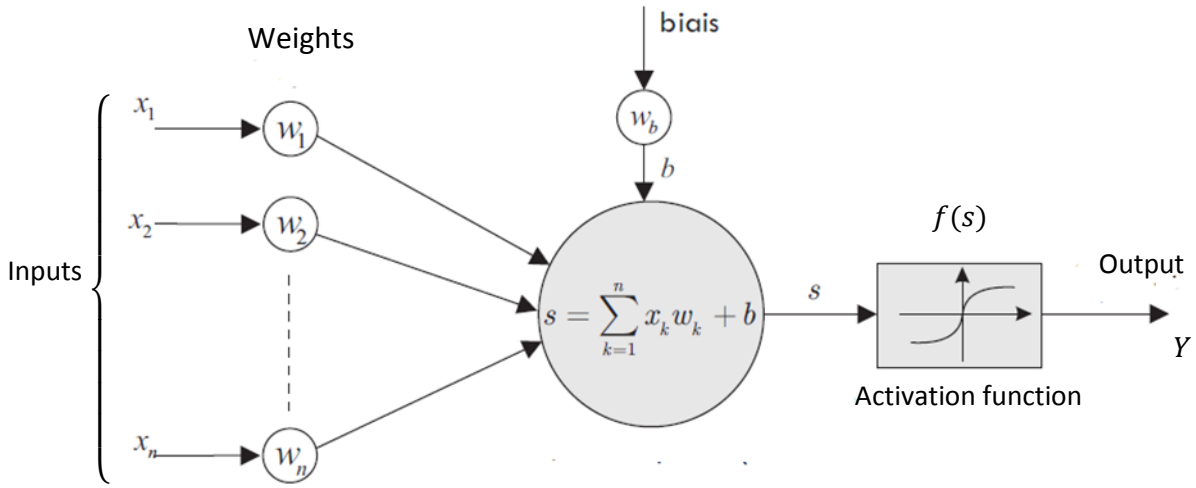

Figure II.6 Model of artificial neuron

With: x_n is the inputs, W_n the weights, b_i the bias, Y the output and *f(s)* the activation function. The most used activation functions are schematized in figure II.7.

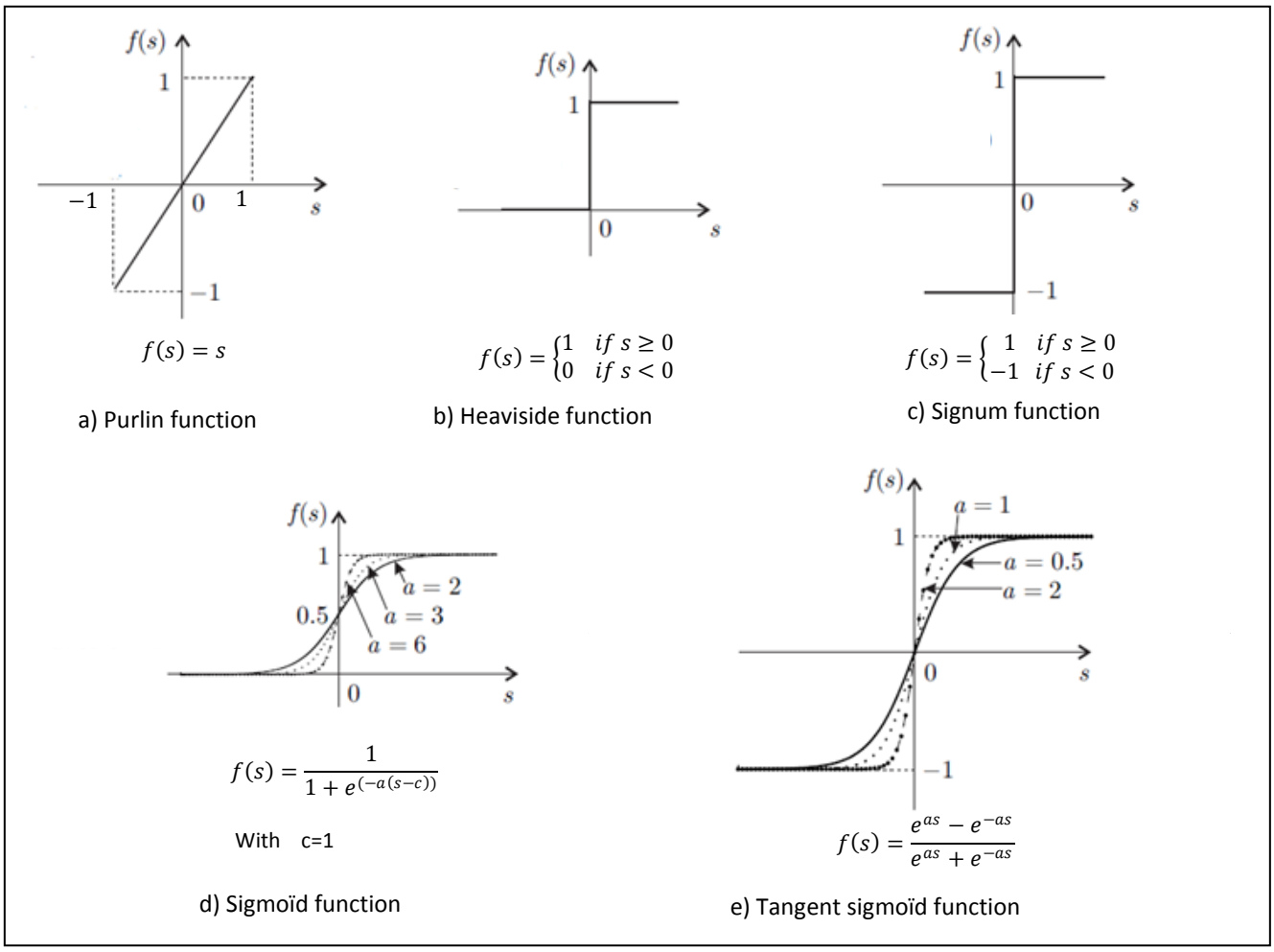

Figure II. 7 Most used activation functions

The output is given by the expression below:

$$Y = f(s) = f(\sum_{n=1}^{N} w_n x_n + b) \quad \text{(II.15)}$$

With *N* number of inputs

II.4.4. Neural network types

There are several models of artificial neural networks of which we can cite:

- **Perceptron**

The Perceptron is a self-organizing system proposed by Roosenblatt. Its main purpose is to solve the problem of explaining brain function in terms of brain structure. It has technological applications as a pattern recognition device. It is a supervised learning of binary classifiers that perform calculations to detect patterns or trends in the input data [52].

- **Multilayer Perceptron**

Multilayer Perceptron (MLP),is an extension of the Perceptron model containing one or more hidden layers connected from lower to upper layers (Figure II.8).

The main objective over MLP is to optimize the layers and neurons number for suitable network with sufficient parameters and good generalization for classification or regression task [53].

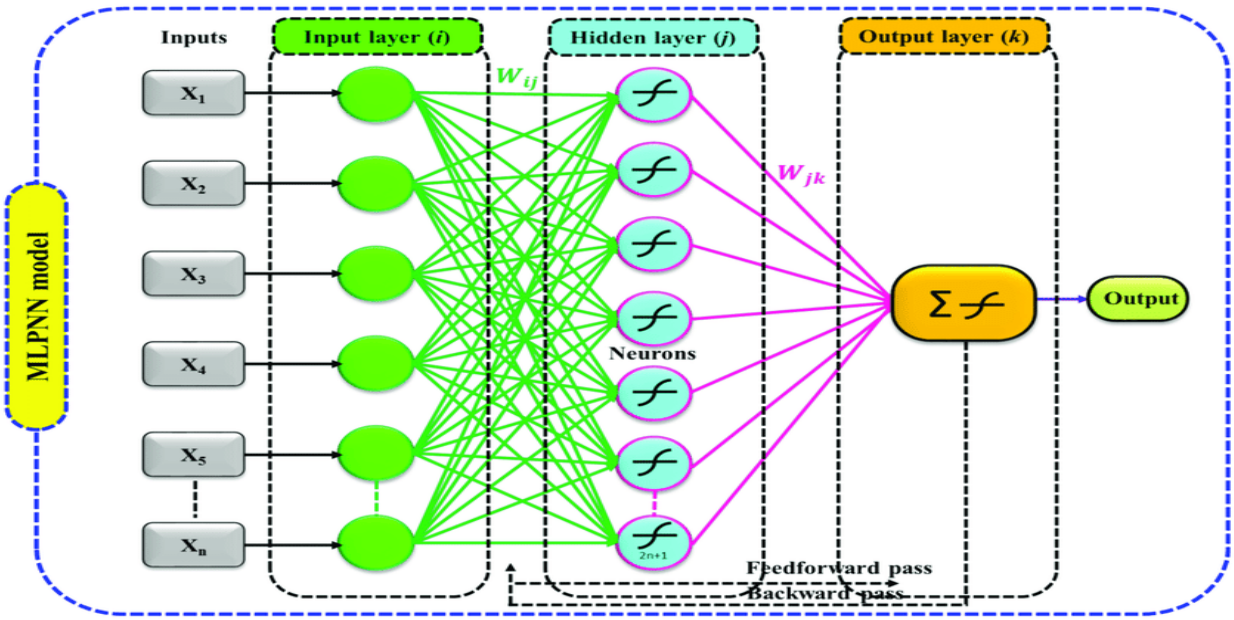

Figure II.8 MLP-NN model [54]

- **Radial basis function**

Radial basis Functions (RBF)surfaced in late 80's as a variant of ANN are embedded in three layers, a nonlinear input, a hidden layer where the unit implements a radial activated function and a linear output where the units implement a weighted sum of hidden unit outputs.

RBF networks has a verity of properties such as localization, functional approximation, interpolation, cluster modeling, quasi-orthogonality and the ability of modeling complex mappings [55].

- **ADALINE**

ADALINE (Adaptative Linear Element) was introduced by Windrow basing on the work of Mcculloch and Pitts. The ADALINE architecture seems to be similar to perceptron one, with a linear activation function[56].

For a problem with *N* inputs, the ADALINE output is expressed as:

$$Y = \sum_{n=1}^{N} w_n x_n \tag{II.16}$$

The ADALINE learning was carried out using Widrow rule that consist of minimizing the quadratic error *Err* [57] :

$$Err = \frac{1}{2}\sum_{n=1}^{N}\left(Ta^{(n)} - Y^{(n)}\right)^2 \tag{II.17}$$

Where: *N* is the total number of training samples; *Ta* and *Y*are respectively the target and calculated outputs correspondents to *N* examples.

- **Convolutional Neural Network**

A convolutional neural network (CNN), is designed for processing structured arrays of data such as digit and images. It is composed of convolutional layer and a fully connected layer, which is the final layer, feeded to the NN and a pooling step that reduces the activation map dimensions, keeping only the important data [58].

- **Probabilistic neural network**

A Probabilistic Neural Network (PNN) is a feed-forward neural network composed of four layers: input layer, pattern layer, summation layer and output layer.

It can estimate the probability density function of a given group of data. PNN is used for classification, using a statistical memory-based approach, and pattern recognition, using kernel functions.

The PNN is based on the concept of traditional probability theory, such as Bayesian classification and other estimators for probability density functions, to build a neural network for classification [59].

- **Hopfield neural network**

Hopfield neural network introduced by Dr. John J. Hopfield in 1984 is a symmetrical, fully connected, two-layer recurrent network that acts as a nonlinear associative memory and is particularly efficient at solving optimization problems. The network is only suitable for bipolar or binary inputs and implements energy functions. Learning is performed by setting each weight that connects two neurons to the product of the inputs from those two neurons. When an incomplete or noisy pattern is presented, the network responds by getting the internally stored pattern that is closest to the presented pattern [60].

II.4.5. Learning neural networks

Artificial neural networks include three categories of learning [34]:

- **Unsupervised learning**

Used when there is no knowledge of the desired outputs for the given inputs. It is a learning algorithm that adjusts the weight of neural links to maximize the classification quality of the inputs[34].

- **Reinforcement learning**

Used when there is no direct knowledge of the ideal outputs; there is some way to know if the outputs are moving towards or away from the desired output. The weight, in this case, are adjusted randomly [34].

- **Supervised learning**

Where the algorithm trains on a set of labeled data and changes until it is able to process the data set to achieve the desired result. The learning in this case is easier and faster because the

weights are adjusted directly switch the calculated error from the difference between the obtained and the desired outputs [34].

II.5 Scalar indicators

II.5.1. Moments

Traditional scalar indicators or moments make it possible to follow the evolution of a signal[61]. When the signal is represented by a sequence of discrete values $x(i)$, (i = 1,2, ..., N), the statistical characteristics the most commonly used are defined as follow:

- Mean value is the average value of a signal[61].

$$\bar{x} = \frac{1}{N}\sum_{i=1}^{N} x_i \tag{II.18}$$

- RMS (Root mean square)value is an estimator of the average power in vibration system that increases with the severity of the defect [61], [62].

$$x_{RMS} = \sqrt{\frac{1}{N}\sum_{i=1}^{N}(x_i)^2} \tag{II.19}$$

- Skewness parameter measures the degree of asymmetry through its probability density function [62], [63].

$$x_{skew} = \frac{\sum_{i=1}^{N}(x_i-\bar{x})^3}{N\sigma^3} \tag{II.20}$$

with σ is the standard deviation.

- Crest factor measures the spikiness and the impulsions of a signal [62], [63].

$$x_{CF} = \frac{x_{peak}}{x_{RMS}} \tag{II.21}$$

- Kurtosis measures whether the data are peaked or flat relative to a normal distribution (Figure II.9) [63].

  A signal's kurtosis is determined by the fourth order moment of the amplitude distribution; defined as:

$$x_{ku} = \frac{\sum_{i=1}^{N}(x_i-\bar{x})^4}{N\sigma^4} \tag{II.22}$$

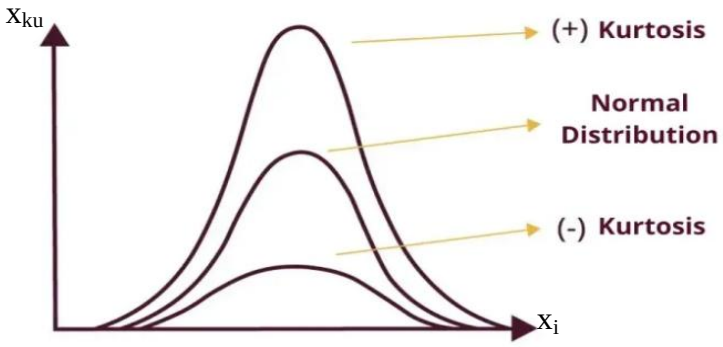

Figure II.9 Kurtosis measurement

II.5.2. L-moments

In 1990, Hosking introduced an extended form of traditional scalar indicators (moments) called L-moments defined as [64], [65]:

$$L_r = r^{-1} \sum_{k=0}^{r-1} (-1)^k \binom{r-1}{k} E(X_{r-k:r}) \qquad r = 1,2,3 \ldots \tag{II.23}$$

The first order l-moment (L_1) defines the L-location parameter, represented as follow:

$$L_1 = E(X_{1:1}) = E(X) \tag{II.24}$$

E(X) is the anticipated value of the variable X.

The second L-moment (L_2) is the L-measure for the dispersion of the distribution.

$$L_2 = \frac{1}{2} E(X_{2:2}) - \frac{1}{2} E(X_{1:2}) = \frac{1}{2} E(X_{2:2} - X_{1:2}) \tag{II.25}$$

The third L-moment (L_3) provides the L-measure for the asymmetry of the distribution of X.

$$L_3 = \frac{1}{3} E(X_{3:3}) - \frac{2}{3} E(X_{2:3}) + \frac{1}{3} E(X_{1:3}) \tag{II.26}$$

The ratio of the second to the first L-moments is called the L-coefficient of variation ($L - cv$).

$$L - cv = \frac{L_2}{L_1} \tag{II.27}$$

The $L -$ Skewness, obtained by division between the third and the second L-moments.

$$L - \text{Skewness} = \frac{L_3}{L_2} \tag{II.28}$$

The *L-kurtosis*, defined as division between the fourth and the second L-moments[66].

$$L - kurtosis = \frac{L_4}{L_2} \tag{II.29}$$

II.6 Conclusion

After the explanation of time-frequency methods throughout this chapter, it seems clear that the wavelet packet decomposition represents the best time-frequency tool for signal processing and fault diagnosis. It is for this reason that we have exploited this method combined with the multilayer perceptron neural networks, the most used for classification, in order to diagnose a set of defects of an induction motor, by exploiting vibration signals and stator currents; all this will be explained and detailed in chapters 3 and 4.

Chapter III

Diagnosis of bearing defects by vibration analysis

III.1 Introduction

Since the performance of IM machines heavily depends on the application of appropriate maintenance methods, the intensive development in the diagnosis and faults detection in these machines has motivated many researchers to work on these issues to keep machines in proper operation to avoid damages and downtimes. Due to a number of factors, bearing defects account for 40 to 50 percent of induction machine failures. These defects may appear on the rolling element bearing inner and outer races, balls, and cages as a result of wear, incorrect lubrication, overheating, wrong mounting, poor bearing selection, faults in the bearing material, and manufacturing errors that alter vibration signatures. Thus, the prognosis of bearing defects has been the focus of numerous research investigations in past few years [67], [68]. Because vibration signals analysis techniques provide significant defects data, they are used in the majority of studies analyzing bearing problems, emphasizing on the time domain [69], [70], frequency domain, such as the Fourier transform, and time–frequency domain techniques in signal processing. The time-frequency technique, particularly the wavelet transform, has gained popularity in recent years. This is because both stationary and non-stationary signals can benefit greatly from the variable width analysis window's excellent time-frequency analysis. In contrast to the Short-Time Fourier Transform (STFT), which faces the issue of resolution when the window's width is left fixed. Choosing a narrow window results in good time and bad frequency resolution, and vice versa, if a wide window is chosen, poor time and excellent frequency resolution. As it allows the decomposition of all frequency sub-bands, improvements in Multi-Resolution Analysis (MRA) have made substantial progress in the theory and application of Wavelet Packet Decomposition (WPD) in the field of fault diagnosis [15], [70-73]. Because it makes it possible to break down all frequency sub-bands. Since they provide accurate information on the faults, Wavelet Packet Transform (WPT) coefficients can be employed directly as characteristics or indicators. Energy, for example, and other WPT coefficient-related data can also be employed as indicators [13], [75]. On the other hand, a number of intelligent classification systems, including support vector machines (SVM) [76], [77], artificial neural networks (ANN)[78], and adaptive neural-fuzzy inference system [79], have been created and used for monitoring and diagnostics. In nowadays, a lot of studies[28], [80], [81] have combined time-frequency and intelligent classifier algorithms while employing conventional scalar indicators. This makes it feasible to track the development of a signal-derived variable used as an input by AI classifiers, such as the WPT coefficients. However, Sellito used L-moments (L-skewness, L- variability, L-

kurtosis,...), an extended variant of conventional moments (skewness, variability, kurtosis, etc.), in his study [82]. Whereas in [66] based on prior research, the author confirmed the efficiency of kurtosis above other traditional vibration characteristics. Some documented literature [81-86] has conducted experiments on fault diagnostics utilizing L- kurtosis and confirmed its superiority over Kurtosis technique on a number of common signals due to several drawbacks. The key benefit of L-kurtosis over kurtosis is that the estimated parameters are more precise and robust to outliers in the data.

Despite these findings, it is clear from the literature that there hasn't been much attention paid to the issue of defect identification of rolling element bearings in particular, mainly in terms of diagnosis using L-kurtosis as an input for Neural Network Classification. Therefore, in the present paper, L-kurtosis is introduced as a new vibration analysis feature and propose a method for diagnosing and classifying defects in rolling bearings using an intelligent classification system. This classifier is based on Multi-Layer Perceptron Neural Networks (MLP-NN) and the wavelet packet decomposition (WPD). The coefficients of the WPD will be used to extract the indicators while energy and L-kurtosis will train the Neural Network. The classification performance of the proposed technique is evaluated and discussed. In this paper the main motivation and contribution with the theoretical background of bearing defects, WPD, Energy and L-kurtosis are explained and detailed. Then the proposed methodology and data acquisition (vibratory signals) are described. Finally, the proposed method is applied to different and combined faults to verify its effectiveness and the obtained results are discussed, then a comparison with recent procedures of bearing defect diagnosis is given.

III.2 Motivation and contribution

Numerous papers have recently emphasized on diagnosing bearing faults using an AI classifier and new features extraction techniques [21], [81], [89], [90], [91], [92], [93], [94]. Regardless, the effectiveness of the chosen procedures and features that provide more details about the type of defects determines how well the proposed procedure will perform. Therefore, a novel combination of features for bearing element problem identification is introduced in this work. The following are the main contributions and motivations of the present work: (1) The classification of impacted rolling element bearings that have not been widely considered, such as poor lubrication, lack of lubrication, and combination of broken cage and lack of lubrication. (2) In addition, a novel feature (L-kurtosis) extracted from WPD coefficients was employed for training an ANN classifier. Using an experimental set-up for data acquisition

(vibratory signals) at different speeds, the proposed method is validated.

III.3 Proposed Methodology

The flowchart depicted in Figure III.1 outlines the proposed methodology introduced in this paper, comprising three essential and crucial stages:

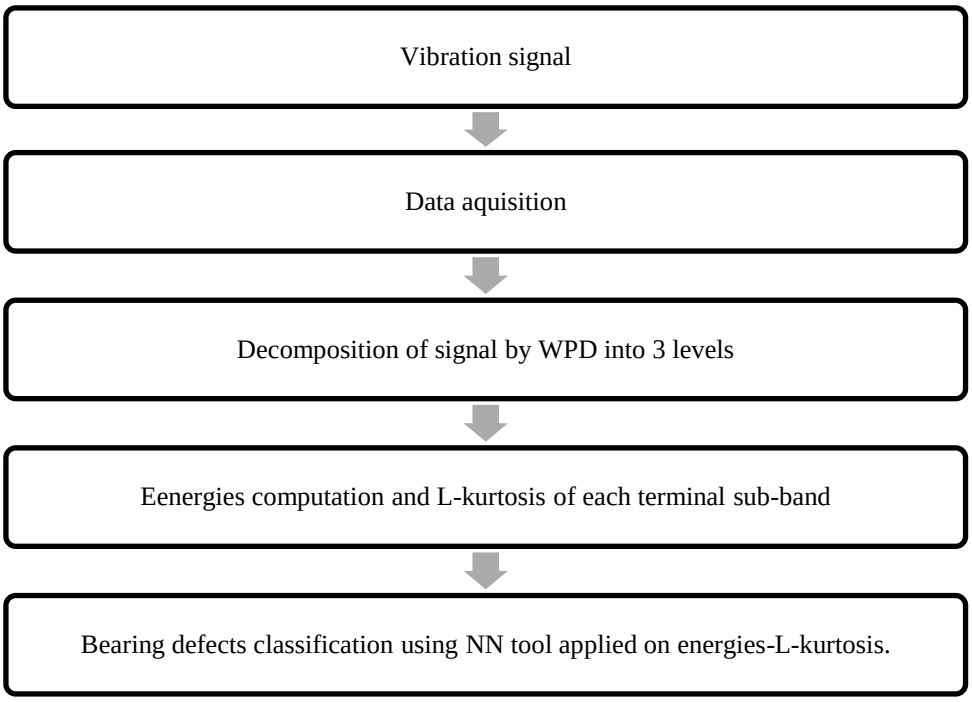

Figure III.1 The proposed methodology

Step 1: Wavelet packet transform (WPT) decomposes signals into three levels using Daubchies mother wavelet (db6), with level 3 being the best suitable for fault diagnosis of bearing problems, according to S. Djaballah and al. [22].

The signal is divided into low and high frequencies at each level using a low pass filter and a high pass filter, respectively. The experimental setup's maximum sampling frequency of 8 KHz is utilized in the current work, resulting in a maximum reconstructed bandwidth of 4000 Hz. The bandwidth used by each packet in this scenario for a depth of 3 corresponds to 500 Hz, as shown in Figure III.2 in accordance with equation (III.1) that represents the maximum value of each node[95].

$$\omega(j,n) = \left(\frac{n+1}{2}\right) * \left({f_s}/{2^j}\right) \quad \text{(III.1)}$$

With: j: decomposition level, n: node and f_s: sampling frequency.

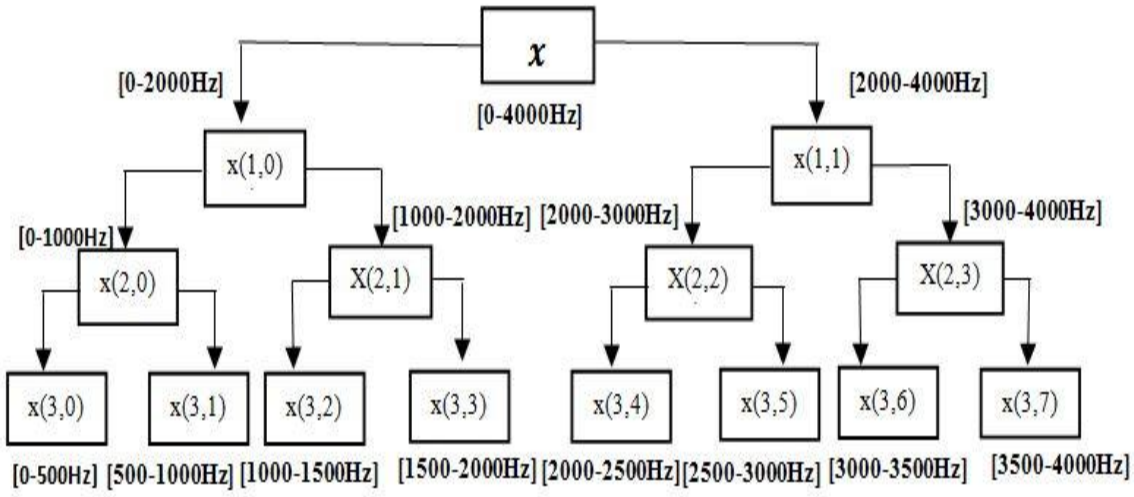

Figure III.2 WPD tree with depth of 3

Step 2: Indicators computation (energy and L-kurtosis) for the third level coefficients obtained from step 1.

* Energy computation

Each sub-band signal's energy level correlates directly with the severity of the defect and is therefore regarded as an indicator of the bearing condition. Thus, the equation written below [13], [79] defines the energy in each sub-band at a decomposition level (j):

$$E_j^n = \int \left| x_j^n(t) \right|^2 dt \tag{III.2}$$

With $x_j^n(t)$ are the wavelet packet coefficients

Similarly, when the signal is represented by a sequence of discrete values $x(i)$, (i = 1,2, ..., N), the energy is computed as shown by the following equation:

$$E_j^n = \sum_{i=1}^{N} x_j^n(i)^2 \tag{III.3}$$

* L-Kurtosis computation

Hosking introduced the L-kurtosis as an alternative distribution character measure in 1990 [96]. It is derived from Sellitto's L-moment[82]. The fourth order L-moment (L-kurtosis), mentioned in chapter 2 is related to L_4 and L_2 quantities given by:

$$\text{Where:} \begin{cases} L_4 = 20\beta_3 - 30\beta_2 + 12\beta_1 - \beta_0 \\ L_2 = 2\beta_1 - \beta_0 \end{cases} \tag{III.4}$$

With β_0, β_1 , β_2 and β_3 coefficients, computed as following equations:

$$\begin{cases} \beta_0 = N^{-1} \sum_{i=1}^{N} x_i \\ \beta_1 = N^{-1} \sum_{i=2}^{N} x_i \left[\frac{(i-1)}{(N-1)}\right] \\ \beta_2 = N^{-1} \sum_{i=3}^{N} x_i \left[\frac{(i-1)(i-2)}{(N-1)(N-2)}\right] \\ \beta_3 = N^{-1} \sum_{i=4}^{N} x_i \left[\frac{(i-1)(i-2)(i-3)}{(N-1)(N-2)(N-3)}\right] \end{cases} \quad \text{(III.5)}$$

Step 3: Classification of bearing faults using MLP-NN, with combination of energy-L-kurtosis as input

III.4 Data acquisition

The measurement setup shown in Figure III.3 is used to acquire data (vibratory signals). A typical cage induction machine (0.37 kW; 1 pole-pair; 380 V; 1.1A) with an encoder, a PC, a USB measuring device, an accelerometer, an elastic claw coupling, a vibration analyzer, a bearing unit, a balanced flywheel (load). The control unit with a frequency converter has the role of gradually adjusting rotational speed. Additionally, the control device has indications for the rotational speed and absorbed motor power. The vibration signals are measured at sampling frequency of 8 KHz, for three rotational speed 500 rpm, 1000 rpm and 2000 rpm, under four different operating situations, healthy case, improper lubrication (IL) (lubricant + humus), lack (absence) of lubrication (LL) and a combination of two faults (lack of lubrication + broken ball cage) (LLBC) as shown in Figure III.4. The parameters of the bearing geometry are indicated in Table III.1.

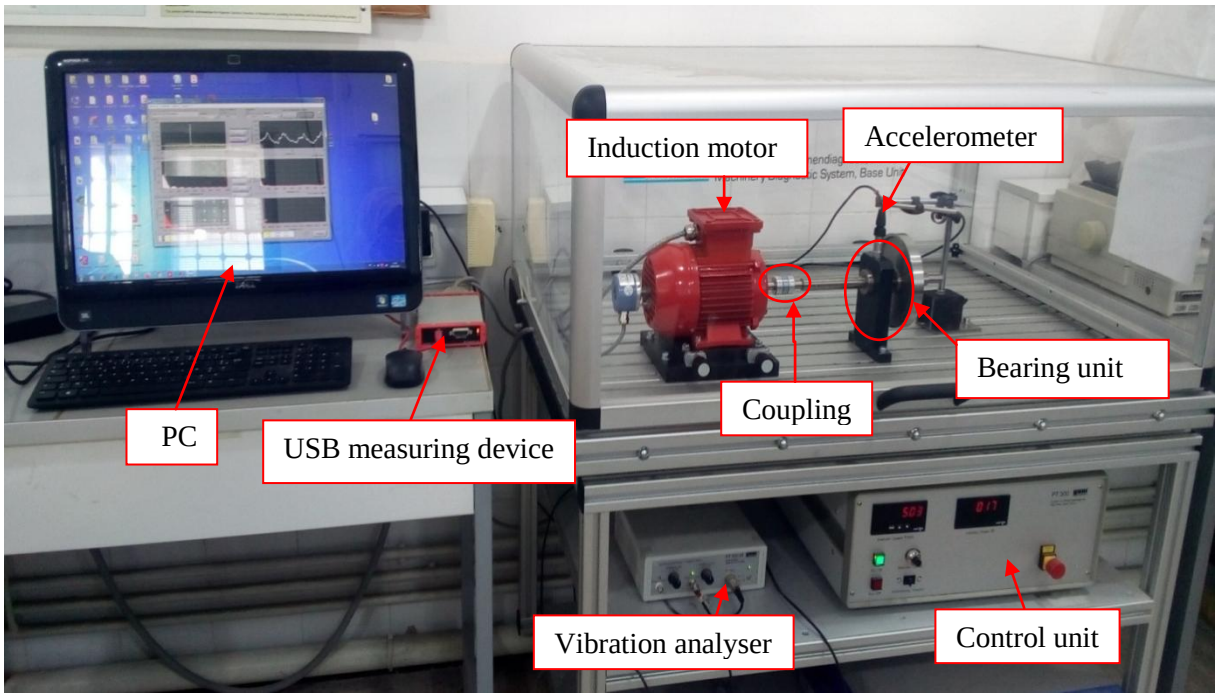

Figure III.3 Experimental setup for bearing vibration signal acquisition

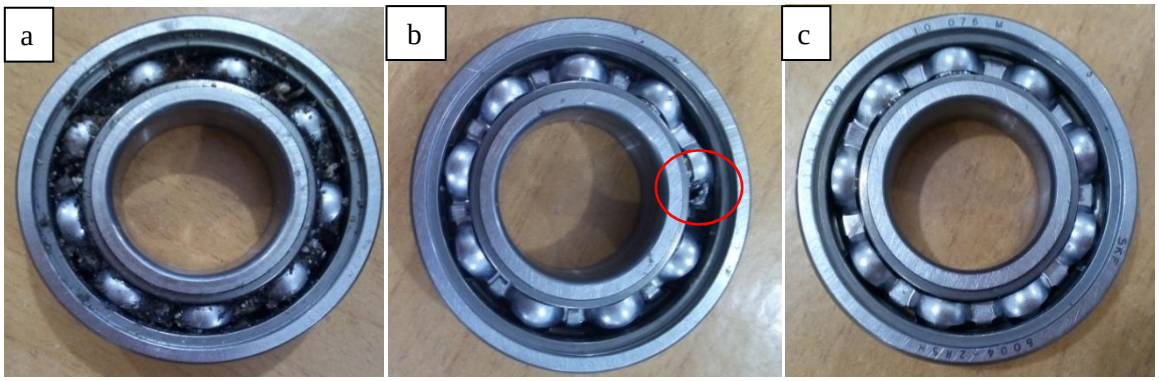

Figure III.4 Bearing defects: a) improper lubrication, b) combination of lack of lubrication and broken bearing cage, c) lack of lubrication

Table III.1 Bearing parameters: ball bearing 6004-2RSH SKF

Inside diameter (mm)	Outside diameter (mm)	Thickness (mm)	Ball diameter (mm)	Pitch diameter (mm)	Number of balls
20	42	12	6	31	9

III.5 Results and discussions

First, a set of vibratory signals was acquired under different states (Figure III.5) using an accelerometer. The coefficients obtained by WPD at a depth of 3 are then calculated using the wavelet Daubchies 6 (Figure III.6) to create the inputs (energy and L-kurtosis).

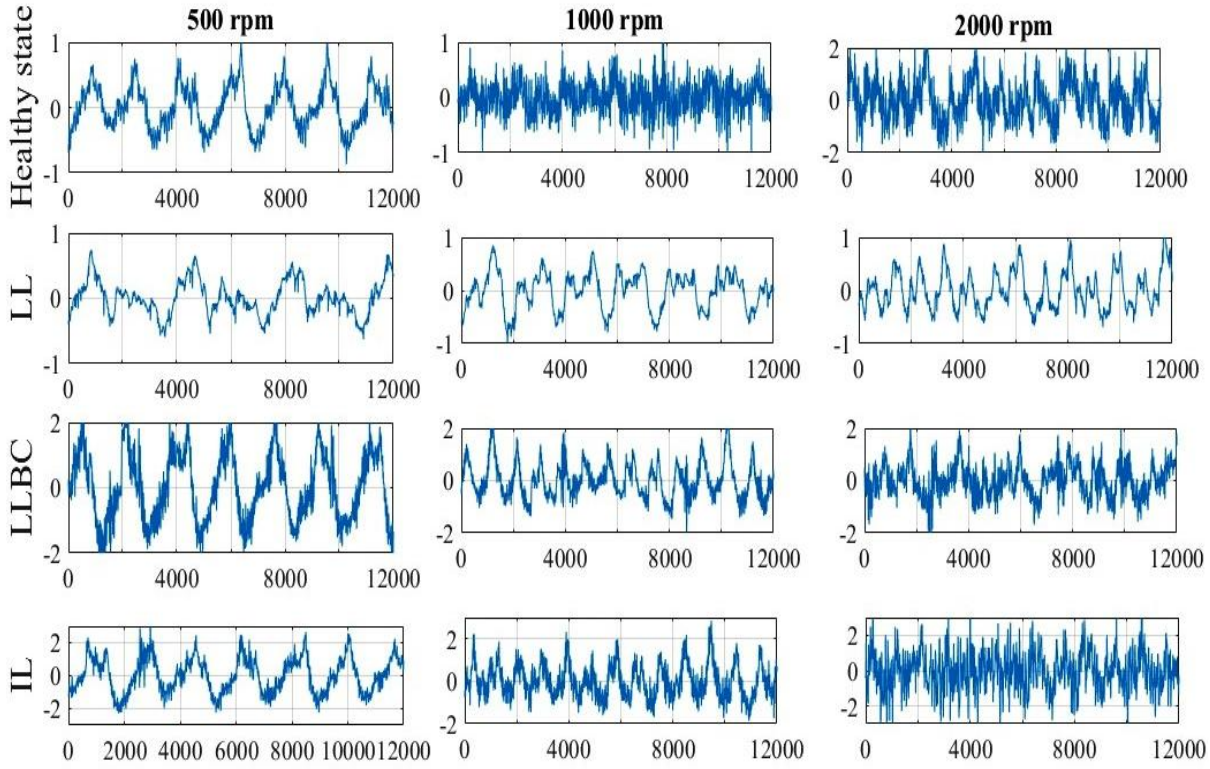

Figure III.5 Example of experimental vibratory signals in different cases

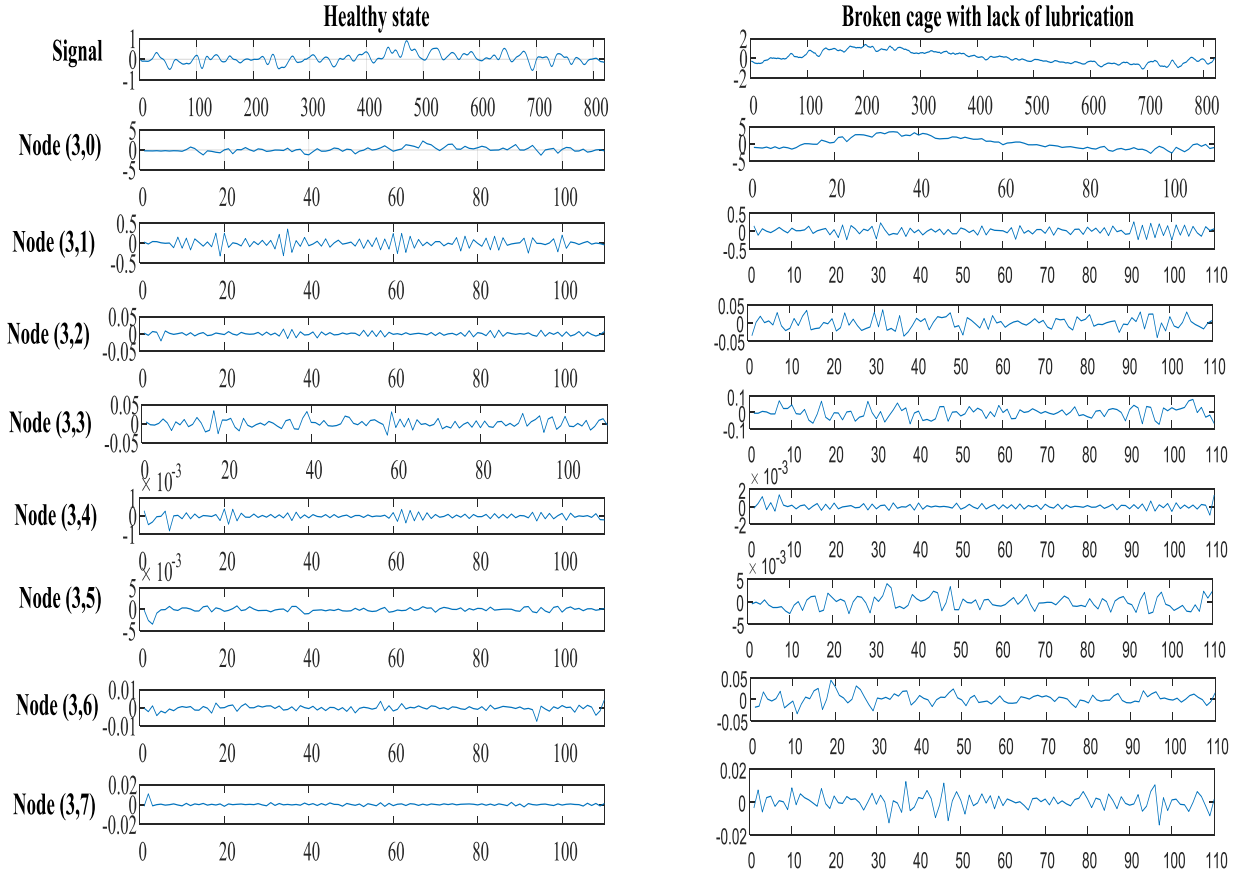

Figure III.6 Original signal and terminal sub-bands in healthy and faulty case

Finally, Multi-Layer Perceptron Neural Network is used to diagnose and classify bearing faults (MLP-NN). For the categorization of bearing faults, the MLP-NN is used. Table III.2 provides a summary of the MLP-NN design parameters.

Table III.2 MLP-NN design parameters

Network input distribution	
Training	[108 signals for each case with 820 samples for each signal] 70%
Testing	[48 signals for each case with 820 samples for each signal] 30%
Learning type	Supervised
Activation function	
Hiden layer	Tangent Sigmoid
Outputlayer	Purlin
Performance	MSE
Weights initialization	Random
Stopped criteria	
Minimum gradient	10^{-7}
Maximum Epochs	1000
Mu	0.001
Inputs	$[E_3^0, E_3^1, E_3^2, E_3^3, E_3^4, E_3^5, E_3^6, E_3^7, LK_3^0, LK_3^1, LK_3^2, LK_3^3, LK_3^4, LK_3^5, LK_3^6, LK_3^7]$

The MLP-NN classifier is depicted in Figure III.7. It is made up of an input layer with 16 inputs, a single hidden layer with 20 neurons, and an output layer. The number three denotes the amount of bit binary code required to encode the various classes taken into consideration in this work, as shown in Table III.3.

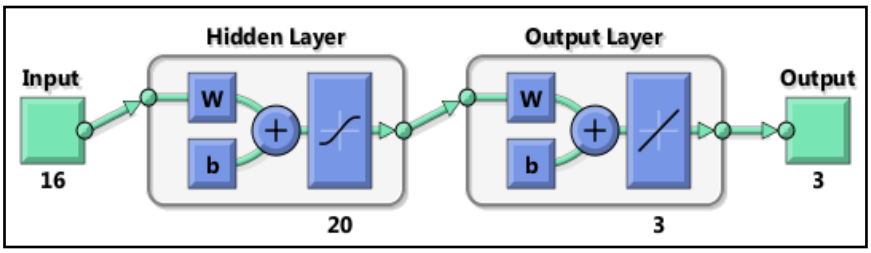

Figure III.7 MLP-NN architecture

The performance rate is calculated by dividing the total number of classification tests by the number of correct classifications:

$$t_r\% = \frac{N_c}{N_t} 100 \quad \text{(III.6)}$$

N_t is the total number of tests, and N_c is the number of correctly classified samples.

The vibration signal is measured at an 8 KHz sampling rate. In this case, database signals are chosen for various shaft rotor speeds and bearing conditions (Normal, IL, LOL, and LOL + BBC) (500 rpm, 1000 rpm and 2000 rpm). Consequently, four categories of faults (Figure III.8) are taken into account and categorized in accordance with Table III.3.

Table III.3 Bearing defects codification

Bearing conditions	**Class**	**Code classes**
Normal	1	000
IL	2	100
LL	3	010
LLBC	4	001

Healthy case (normal), improper lubrication (IL) (lubricant + humus), lack (absence) of lubrication (LL) and a combination of two defects (lack of lubrication + broken ball cage) (LLBC).

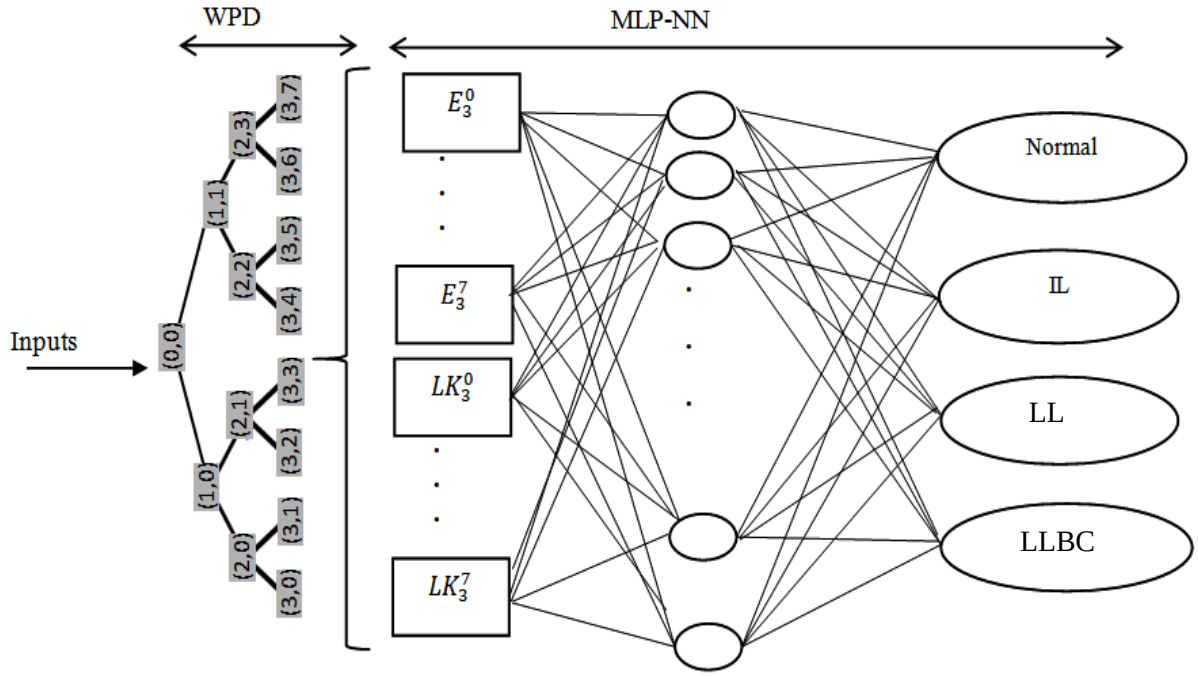

Figure III.8 ANN classifier structure with 4 classes

Figure III.9 and Figure III.10, Represent the regression line and the classification results of bearing defects using energy-L-kurtosis indicators as inputs respectively.

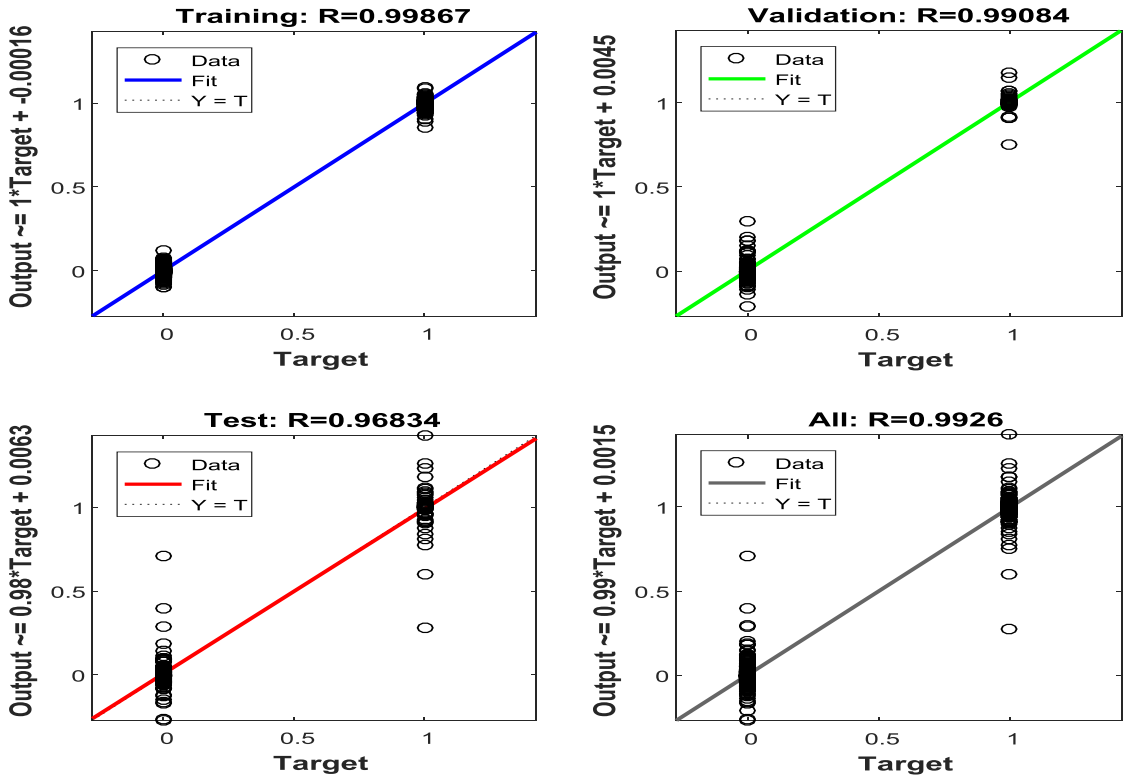

Figure III.9 Regression line of training MLP-NN

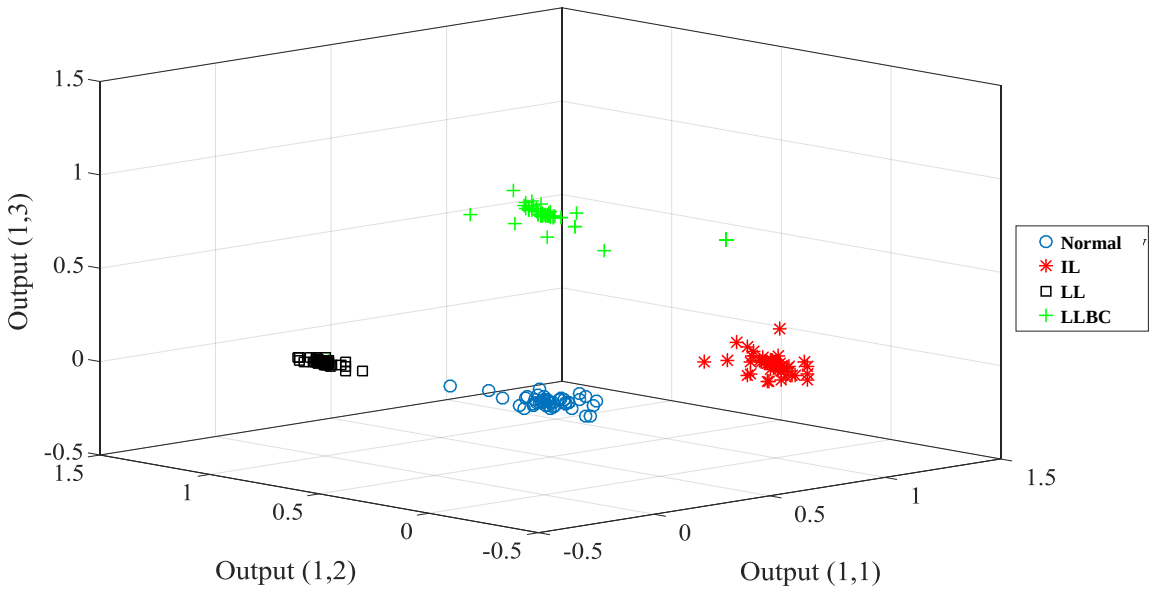

Figure III.10 Rolling defects test set classification using energy-L-kurtosis indicator

Table III.4 Classification performance

MLP-NN		Regression	Performance rate t_r(%)
Number of inputs	**Number of classes**		
16	4	0.9926	99.47

Table III.4 lists the indicators used to create the input vectors, the classes involved, the total number of regressions, and the performance the algorithm achieved utilizing the inputs from the "Energy-L-Kurtosis" pair. The accuracy of the suggested method in classifying faults above other previously used methods is demonstrated by the Neural Network performance when classifying test set data into the 4 classes, which is equal to 99.47 percent. This is as a result of its resistance to outliers. These results demonstrate the effectiveness of the suggested approach to enhance the classification of bearing faults even when the speed is altered significantly.

III.6 Comparison with recent literature of bearing defect classification

In order to illustrate the potential application of the proposed method, a comparative study on the current work and several defect diagnostic techniques are discussed.

The works carried out on the bearing defect classification focuses on the common defect types that are outer race, inner race, cage and ball defects; these works can be found in[27], [89-93], [96-99] that proved their higher performances; but these researches are based on complex feature extraction procedures. For example, in [90] Attoui and al. proposed a long algorithm that includes four key steps: data acquisition, feature generation, feature selection, and defect classification. For this, they employed, while basing on the envelope model, the following methods: the DWPT (discrete wavelet packet transform), the FFT (fast Fourier transform) and the ANFIS (Adaptive Neuro-Fuzzy Inference System). The same for Huibin Zhu and al. [97] as they proposed combined methods called wavelet packet transform- Multi-Weight Singular Value Decomposition (WPT-MWSVD) to extract entropy value for Support Vector Machine training. The methodology of Niloofar Gharesi and al.[91] is based on generalized discriminant analysis for feature extraction, and WNN (Wavelet Neural Network) for classification with no load or speed variation which is the case of the research work presented in [100]. In [28] Pavan Agrawal and al. have combined between Continuous wavelet coefficients and support vector machine; but, as in [98], [99] they used more than six

statistical indicators to train the classifiers. The researchers in [92] have applied a model, based on mathematical matrixes, called graph modeled singular values besides to Kernel Neural Network for bearing defects classification. Zhuyun Chen and al.[93] and Amrinder Singh Minhas and al. [94] have achieved a good performance of 98.93% and 98% respectively while using more simple feature extraction methodologies.

The present research [101] aims to identify different impacted element bearing cases such as poor lubrication, lack of lubrication, and combination of broken cage and lack of lubrication with different rotational speed 500, 1000 and 2000 rpm. The experimental results confirm the high performance of 99.47% in identifying several bearing defect types for only 2 features, energy and L-kurtosis, which have not been used before as an indicator for classification, employing only wavelet packet decomposition as a feature extraction method and MLP-NN as classifier.

III.7 Conclusion

This work investigates a combined WPD and ANN technique to increase the accuracy of IMs bearing defects detection and classification. For a variety of faults and faults severities, vibrational signals acquired by experimental setup are decomposed using the WPD. In order to classify bearing faults, two indicators, energy and L-kurtosis of each terminal third level sub-band are computed. The findings validated the performance of the suggested strategy when L-kurtosis is used as an indicator for bearing defect detection. Additionally, the proposed MLP-NN provided a greater classifying percentage, nearly perfect accuracy, and performance for bearing faults. It can be said that the proposed methodology can be expanded to find other induction faults.

Chapter IV

Diagnosis of mechanical defects by vibration analysis

IV.1 Introduction

Despite the development, which affects all fields, induction motors remain essential machines in the industrial world, and researchers are constantly investigating these machines and developing diagnostic methods in order to ensure their availability.

Our research in this part aims to address five types of defects, which are not fairly treated in previous researches: load unbalance, parallel misalignment, improper lubrication, lack of lubrication, combined defects of broken cage + lack of lubrication. We present a novel methodology based on the WPD energy, the MLP-NN that, is the easiest and most popular AI technique for its application and the statistical parameter l-kurtosis. The WPD represents the best time-frequency method due to its better resolution over the other time-frequency approaches for ability to decompose both high and low frequencies of the considered signal. The L-kurtosis introduced as simple indicator switch the variation of its values used to indicate the defects such as in [101-103], but not considered previously as a feature of classification despite its precision and its robustness to outliers.

This method is carried out on the vibratory signals of asynchronous motors at two different speeds to detect three main types of defects: bearing faults, load imbalance and misalignment.

The obtained results show the reliability of the proposed method with high accuracy, which encourages its use in the detection of other defects.

IV.2 Vibration technique

Vibration technique is generally used for the detection of mechanical faults, according to the data provided by the vibration signals, using sensors. Thus, there are three types of sensors[8] : acceleration sensors; speed sensors limited to low frequency response; and displacement sensors which are eddy current electrical sensors with non-contact measurement.

The various vibration data acquired are used for the determination and validation of various defects [6] change their frequencies as shown in Table IV.1[4], [44], [105], [106].

Table IV.1 Characteristic frequencies of IM defects on vibration signals

Defect	Additional frequency components of vibration
Bearing defects	$f_i = Zf_r/2\left(1+\frac{d}{D}\cos\alpha\right)$ for inner race defect; $f_o = Zf_r/2\left(1-\frac{d}{D}\cos\alpha\right)$ for outer race defect; $f_b = Zf_r/d\left(1-\frac{d^2}{D^2}\cos^2\alpha\right)$ for ball defect; $f_t = {f_r}^2/2\left(1-\frac{d}{D}\cos\alpha\right)$ for train defect; *Z*: number of rollers/balls, *d*: diameter of the rolling element, *D*: diameter of the pitch circle of the bearing, α: the contact angle in radians, and f_r is the frequency of rotation.
Broken rotor bars	$f_{brb} = f_r \pm f_p$ $f_p = (f_{su} - f_r)p$ f_p: pole passing frequency, *p*: number of poles and f_{su}: supply frequency

IV.3 Description of the test bench

The designed experimental setup (Figure IV.1) is composed from:

- Motor group Composed of a three-phase motor with encoder, it is mounted on the second end of the shaft. The motor is mounted on a base plate with alignment device. This device allows horizontally align the axis of the motor. The motor specifications are: 0.37 kW; 1 pair pole; 380 V; 1.11A;
- USB measuring device consisting of 37-pin D-sub connector for connection to the measuring amplifier and USB Port for PC connection.
- Accelerometer which are piezoelectric sensors with integrated electronic circuit. The sensors convert the vibrations measured in electrical signals. The sensitivity is 100 mV/g, with g in m/s²;
- Vibration analyzer or measurement amplifier supplies the sensors current acceleration and amplifies the signals acceleration sensors. Switches knobs allow you to select the amplification between 1, 10 and 100. Then the signal is digitized in the USB measuring device and transferred to the PC where it is processed. The set amplification factor is also transferred to the PC and displayed in the software.

- Control unit which contains a frequency converter intended to regulate gradually the speed of rotation. The control unit also contains the rotation speed indicator and an indicator for the power absorbed by the motor;
- Elastic claw coupling;
- Bearing unit;
- Balanced flywheel (load);

The vibration signal used in our application, was collected at sampling frequency of 8 KHz, for two rotation speed 1500 rpm and 2000 rpm, under different operating conditions as represented in Table IV.2 and Figure IV.2. The parameters of the bearing geometry are indicated in Table IV.3.

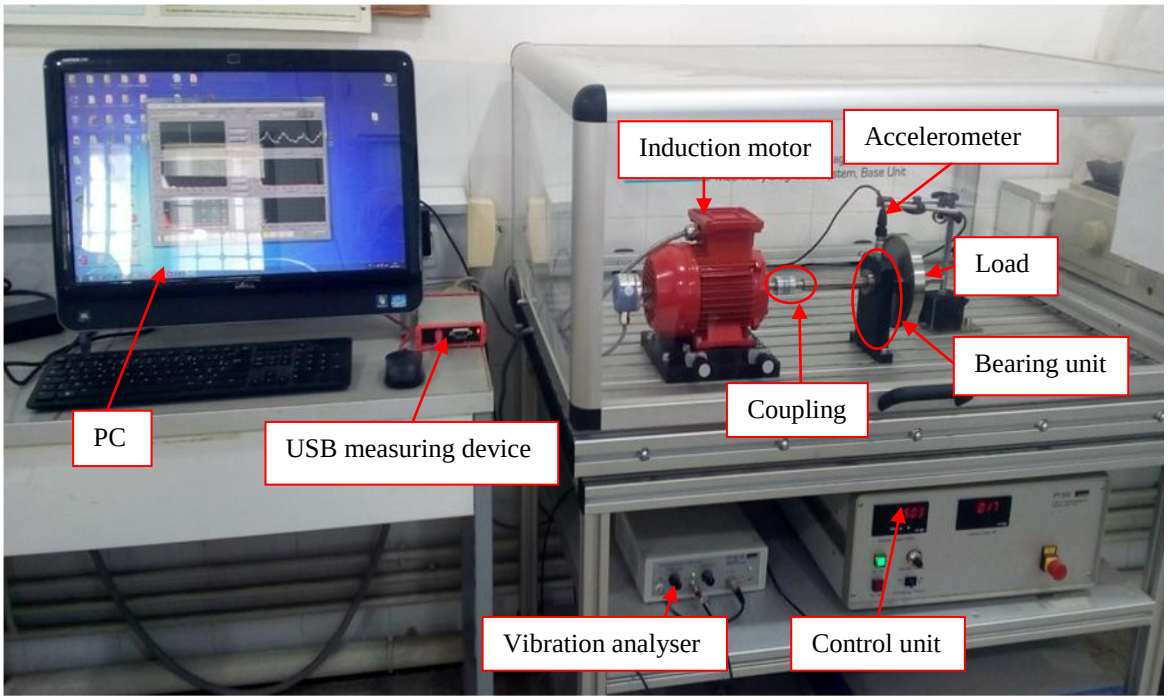

Figure IV.1 Experimental setup

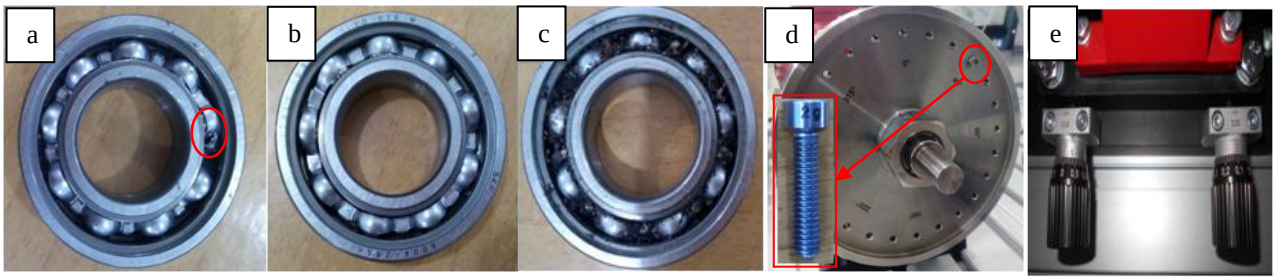

Figure IV.2 IM defects: a) combined defects (lack of lubrication + broken cage), b) lack of lubrication, c) improper lubrication, d) load unbalance, e) parallel misalignment

Table IV.2 Operating conditions of the collected data

		1500 rpm	2000 rpm
Healthy state		✓	✓
Parallel misalignment	0.5 mm	✓	✓
Load unbalance	2 g	✓	✓
Bearing defect	Lack of lubrication	✓	✓
	Lack of lubrication + broken cage	✓	✓
	Improper lubrication	✓	✓

Table IV.3 Bearing parameters: ball bearing 6004-2RSH SKF

Inside diameter (mm)	**Outside diameter (mm)**	**Thickness (mm)**	**Ball diameter (mm)**	**Pitch diameter (mm)**	**Number of balls**
20	42	12	6	31	9

The three defective cases are defined as follow:

- Misalignment

Misalignment is a condition in which the drive machine shaft and the driven machine shaft are not on the same centerline. There are three types of misalignment: parallel, angular and general misalignment, as shown in Figure IV.3 [107].

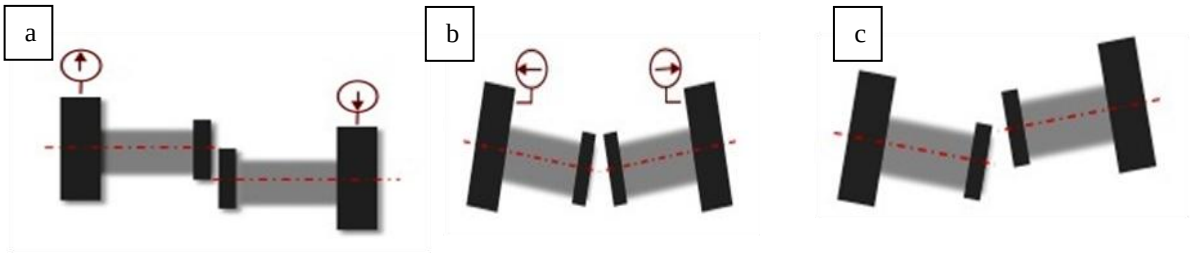

Figure IV.3 Misalignment: a) parallel, b) angular, c) general

- Load unbalance

Load unbalance defect is defined as a non-uniform distribution of the mass around an axis of rotation by placing additional weights on a balanced metal disk (Figure IV.4). This mass provoke a centrifugal force which induces torque oscillations at particular frequencies often linked to the mechanical speed of the motor [13]. Switch [108], within the vibration analysis, the amplitude of the motor speed decreases with the increase of the load.

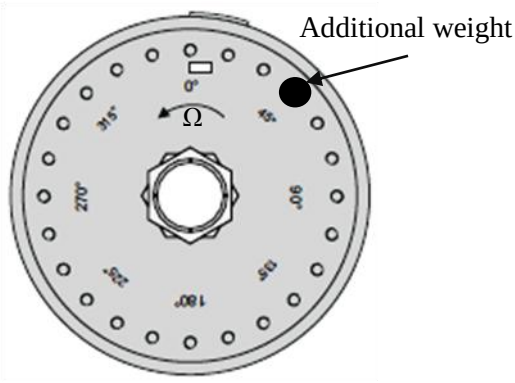

Figure IV.4 Load unbalance

- Bearing defect

The statistical study of IM's defects indicate that bearings failures represent more than forty percent of the IM defects. These defects can be occurred on several components of the rolling element bearing (inner and outer races, rolling elements and cages) as shown in Figure IV.5 owing to several factors such as [6], [105], [109]:

a. Lubrication failure: related to insufficiency, degradation or lubricant impropriety that can lead to bearing overheating.

b. Corrosion and contamination: caused by the insertion of foreign particles into lubricant or deteriorated corrosive solution.

c. Excessive load that means application of load excessively.

d. Incorrect assembly and misalignment: the interference fit mechanism should be used for mounting bearings on rotating rings and the lock nuts must be tight.

Bearing issues appears in additional frequencies that express each type of defect as follows:

$$\begin{cases} f_{OR}\,(Hz) = \frac{Z}{2} f_r (1 - \frac{B_D}{C_D} cos\alpha) \\ f_{IR}\,(Hz) = \frac{Z}{2} f_r (1 + \frac{B_D}{C_D} cos\alpha) \\ f_B\,(Hz) = f_r \frac{C_D}{2B_D} \left[1 - \left(\frac{B_D}{C_D} cos\alpha\right)^2\right] \\ f_c(Hz) = \frac{f_r}{2} (1 - \frac{B_D}{C_D} cos\alpha) \end{cases} \quad \text{(IV.1)}$$

Where: Z: number of rollers/balls, B_D: ball diameter, C_D: pitch circle diameter of bearing, α:the contact angle in radians, and f_r is the rotational frequency.

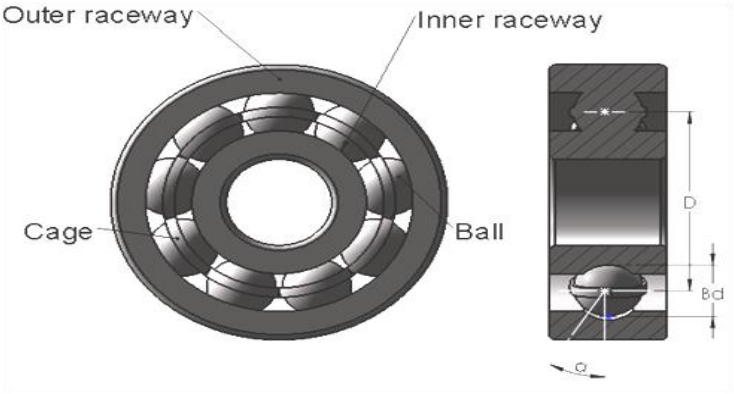

Figure IV.5 Bearing components

IV.4 Proposed methodology

The proposed methodology for this research [110] can be resumed by the flowchart (Figure IV.6). It consists of: (1) decomposition of signals into three levels by WPD using Daubechies mother wavelet (db6). (2) Calculation energies and L-kurtosis of each terminal subband of the third level of the WPD. (3) Classification of IM defects using MLP-NN, by giving energies and L-kurtosis values as inputs.

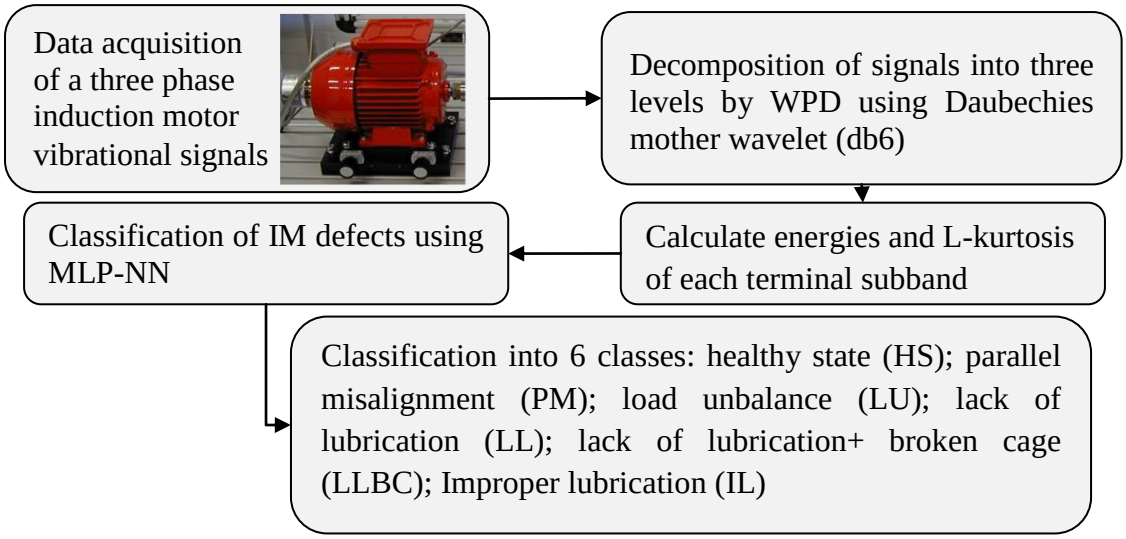

Figure IV.6 Proposed methodology

IV.5 Results and discussion

In order to validate the proposed method, a set of vibration signals obtained from the experimental setup at different operating conditions are exploited. For each case, 12 signals are measured, where each signal is composed from 820 samples. The 144 signals, in total, are decomposed by the WPD using the mother wavelet Daubchies 6 at depth of 3.

Figure IV.7 and Figure IV.8 present the original signal and the eight nodes resultant from the WPD at depth of three, of the two first cases: healthy state and parallel misalignment, at a rotational speed of 2000 rpm.

Through a visual comparison of the two figures, Figure IV.7 and Figure IV.8, we remark that the amplitude of the original signal in the defective state as well as the signals resulting from the wavelet packet decomposition, are much more important than the vibratory signal amplitudes taken from the machine in a healthy state.

The different signals of the nodes are used to extract the values of energies and L-kurtosis in order to train the artificial neural network. Table IV.4 represents some values of the two indicators: energy and L-kurtosis, taken from the same sub-band for each operating condition, we have taken the example of the node (3, 0) where the values are most significant. It can be noticed that the increase in the severity of the defect treated, increases the value of the energy, the same for L-kurtosis, although the value of the energy increases intensively, the value of L-kurtosis varies slowly which prove its robustness to outliers.

These values variations helped the neural network presented in this paper to make the right classification decision.

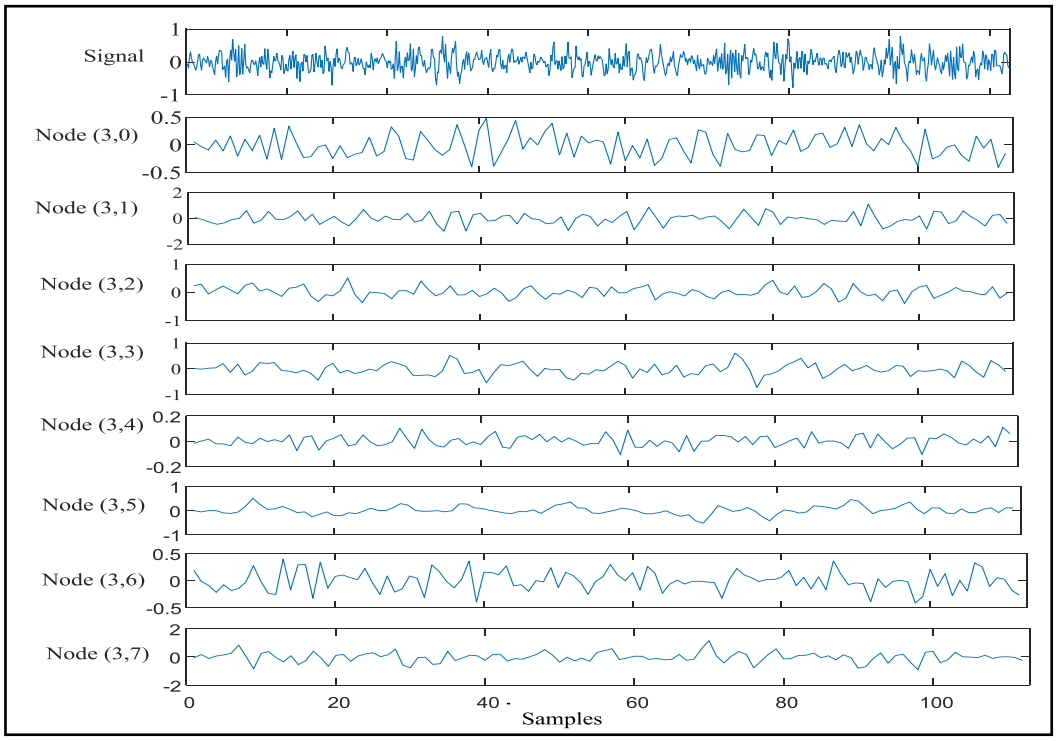

Figure IV.7 Original signal and terminal sub-bands in a healthy state

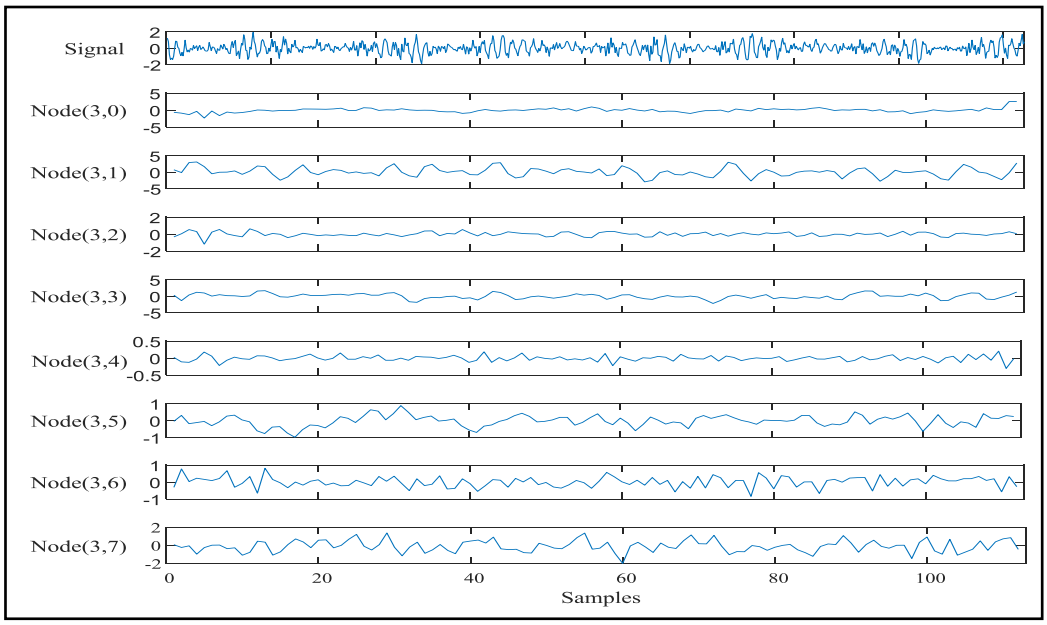

Figure IV.8 Original signal and terminal sub-bands in case of parallel misalignment

Table IV.4 Samples of energy and L-kurtosis values from node (3, 0)

	HS	**PM**	**LU**	**LL**	**LLBC**	**IL**
Energy	5.526	22.542	498.996	59.328	269.487	619.726
L-kurtosis	0.091	0.100	0.137	0.108	0.134	0.144

The indicators, energy and L-kurtosis, calculated from the WPD terminal subbands are introduced to train the Neural Network classifier.

The classification of the IM defects are performed by Multi-Layer Perceptron neural network (MLP-NN) (Figure IV.9). Thus, 96 examples (signals) are used as training inputs and 48 examples as testing inputs, the rest of parameters used for neural networks are grouped in Table IV.5.

Table IV.5 MLP-NN design parameters

Learning type	Supervised
Activation function	
Hiden layer	Tangent sigmoid
Output layer	Purlin
Performance	MSE
Weights initialization	Random
Stopped criteria	
Minimum gradient	10^{-7}
Maximum Epochs	1000
Mu	0.001

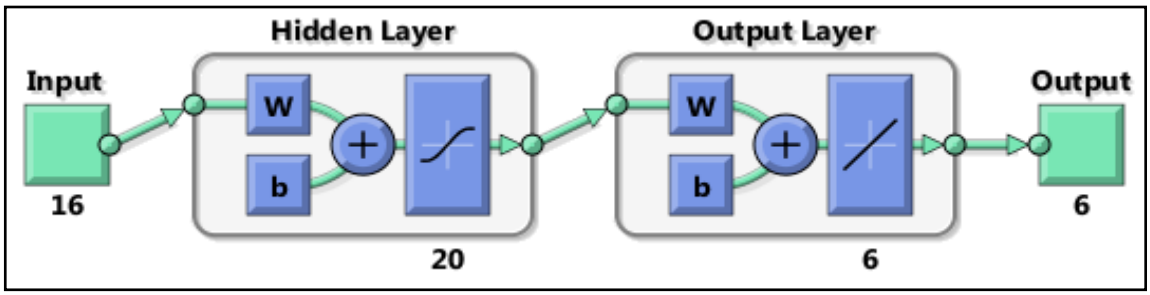

Figure IV.9 MLP-NN architecture

In order to facilitate classification, the studied IM defects are coded as represented in Table IV.6.

Table IV.6 IM defects codification

IM conditions	class	Code classes
HS	1	100000
PM	2	010000
LU	3	001000
LL	4	000100
LLBC	5	000010
IL	6	000001

Figure IV.10 represents the experimental train and test outputs, which shows that the accuracy of the MLP-NN when classifying data according to the types of defects (6 classes) is equal to 100 % with small errors that can be observed by the slight variation in values around the target outputs presented by the code classes in the same order as mentioned in Table IV.6; with a total regression of 0.99893 (Figure IV.11). The regression coefficients indicate that the neural network model performs extremely well on the training, validation and test sets, with slight dispersion of points around the line which indicates good prediction performance, suggesting that the model is well regularized and generalizes well.

The present results confirm the effectiveness of the proposed method for IM defects classification under different load conditions.

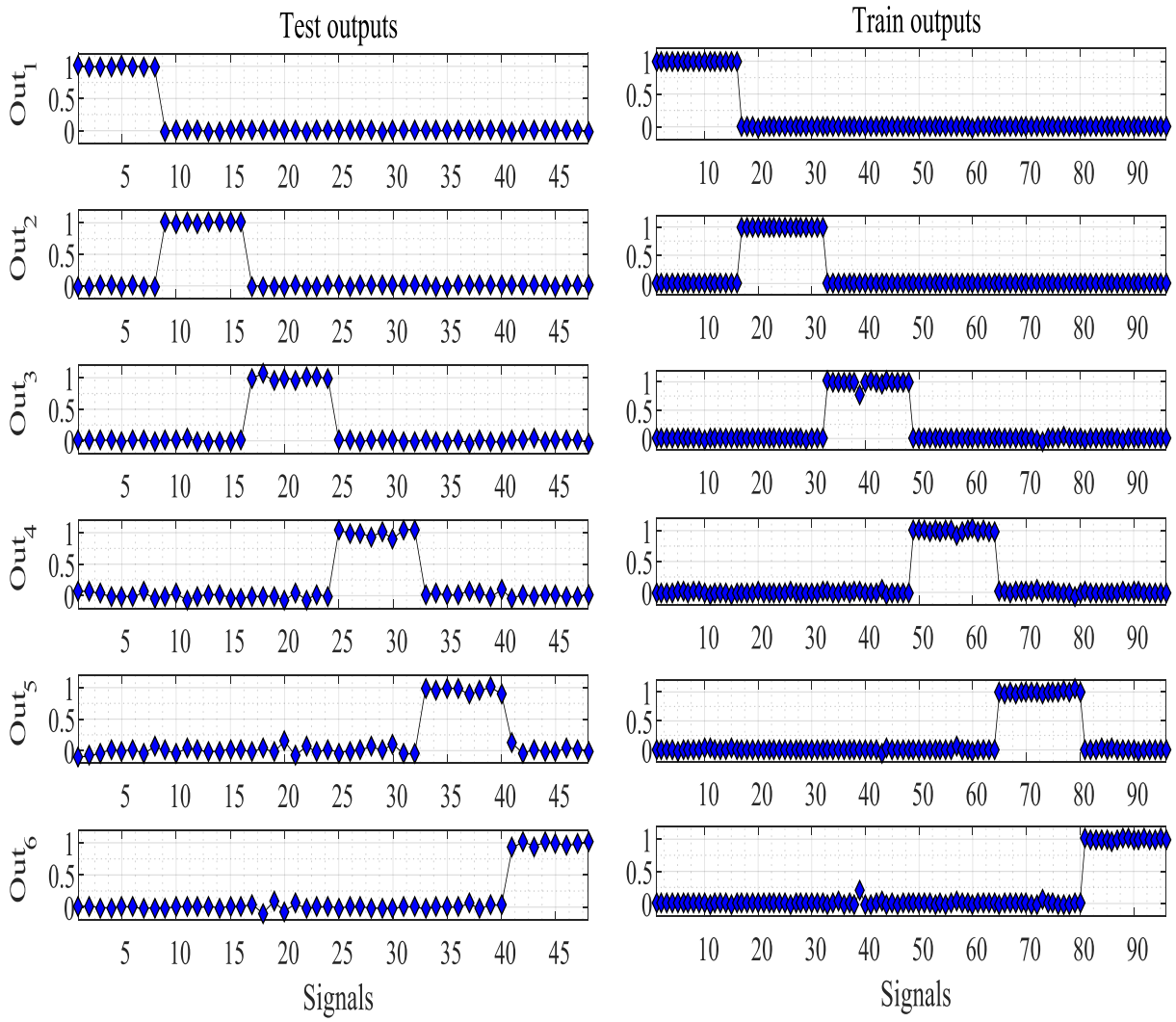

Figure IV.10 Experimental train and test outputs

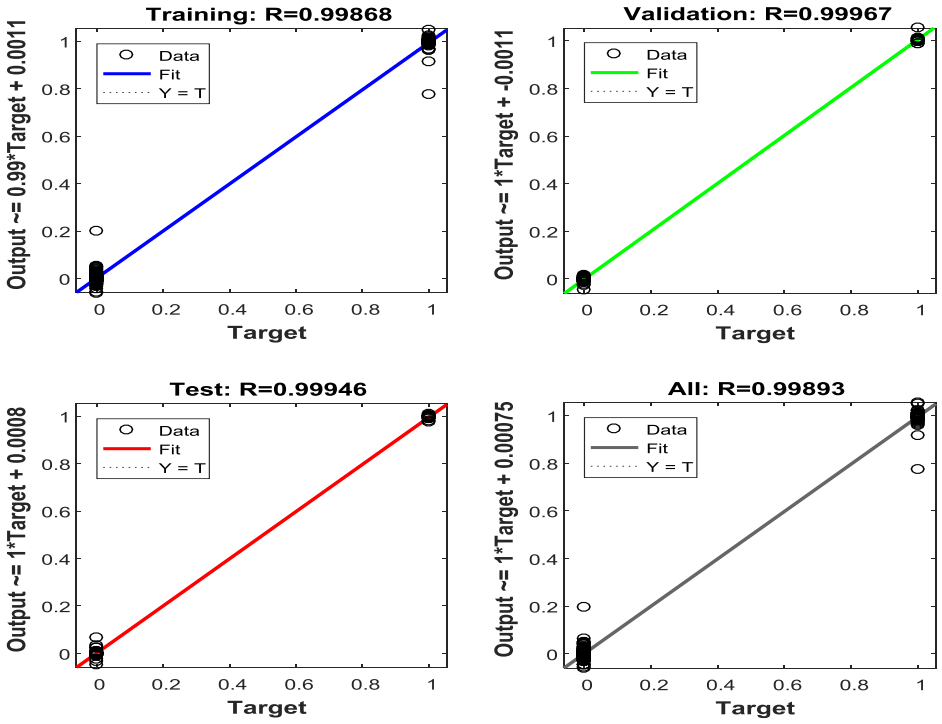

Figure IV.11 Regression line of training MLP-NN

IV.6 Conclusion

This work examined the efficiency of the proposed methodology based on the combination of two methods of different types, the wavelet packet decomposition and the multilayer perceptron neural networks, by introducing the two statistical parameters: energy and l-kurtosis, calculated from each terminal subband of the WPD, as inputs to the classifier.

This methodology was carried out on an induction motor with two different speeds in order to detect three categories of defects: bearing defect, load unbalance and misalignment.

The obtained results show the reliability of the proposed method, which encourages its use for the detection of other defects.

General conclusion and perspectives

Fault diagnosis represents a very important area of research. If the location and time of faults occurring in machines can be detected correctly, then appropriate measures can be taken to avoid further degradation and serious damage to components, and avoid certain safety issues in advance.

This thesis is a continuation of the work on fault diagnosis of AC motors, the main objective of which is to establish a simple and effective methodology based on the time-frequency method for fault diagnosis.

The first chapter presented a bibliographical review of research work carried out on asynchronous motor faults and currently emerging diagnostic methods and techniques.

A general view of the signals and the main time-frequency transformations as well as scalar indicators and artificial neural networks were detailed in the second chapter in order to choose the most suitable combination for our research.

After the explanation of time-frequency methods, it seems clear that the wavelet packet decomposition represents the best time-frequency tool for signal processing and fault diagnosis; it is for this reason that we exploited this technique for diagnosing induction motor faults using vibration signals.

The methodology proposed in our work concerns three different stages that complement each other:

- A time-frequency method represented by wavelet packet decomposition used to facilitate the characterization of motor vibration modes
- The scalar indicator l-kurtosis and energy used to detect changes in the statistical distribution of signals at different scales for different nodes of the wavelet packet decomposition and to characterize the intensity of vibrations at different frequencies and over different time periods of the latter respectively in order to have a reliable classification of the different signals
- The multilayer neural network ultimately used for the classification of the different defects processed

This method is applied for the diagnosis of bearing faults that represents a critical element for motors as mentioned in chapter three.

To validate the effectiveness of the proposed method, chapter four expose a second experimental study was carried out by exploiting several types of faults with two different rotation speeds while improving the operating conditions of the engine, which gave better results.

The results presented in the two works confirm the ability of this method to describe the behavior of the system. These results are associated with and adhere to other parallel work in the context of fault diagnosis of asynchronous motors by analysis of vibration signals.

Our main contributions are summarized as follows:

- Diagnosis of bearing lubrication defects which is one of the main causes of bearing breakage
- Classification of combined induction motor defects that have not been widely studied
- The integration of a new combination of indicators (L-kurtosis and energy) extracted from WPD to train the MLP-NN classifier to diagnose several IM faults
- A data collection system was used to evaluate the suggested methodology at different motor rotation speeds

The perspectives of this work are numerous and obviously require additional developments:

- Exploitation of the proposed methodology to diagnose other types of combined faults
- Exploitation of other combinations of scalar indicators to help identify defects
- Proposal of a shared and reliable method for different types of signals
- Exploitation of other artificial intelligence techniques for fault diagnosis and classification methods
- Consider fault diagnosis of other new renewable energy source equipment and new technologies such as electric vehicles

References

[1] N. Tesla, « Electro—Magnetic Motor », US382279A, 1 mai 1888 Consulté le: 18 juin 2022. [En ligne]. Disponible sur: https://patents.google.com/patent/US382279A/en

[2] N. Tesla, « A NEW SYSTEM OF ALTERNATE CURRENT MOTORS AND TRANSFORMERS », American Institute of Electrical Engineers, vol. 10, p. 308-327, mai 1888.

[3] M. Koteich, « Modélisation et Observabilité des Machines Électriques », Université Paris-Saclay, Paris, 2016.

[4] S. Kumar et al., « A Comprehensive Review of Condition Based Prognostic Maintenance (CBPM) for Induction Motor », IEEE Access, vol. 7, p. 90690-90704, 2019, doi: 10.1109/ACCESS.2019.2926527.

[5] A. Choudhary, D. Goyal, S. L. Shimi, et A. Akula, « Condition Monitoring and Fault Diagnosis of Induction Motors: A Review », Arch Computat Methods Eng, vol. 26, no 4, p. 1221-1238, sept. 2019, doi: 10.1007/s11831-018-9286-z.

[6] C. Malla et I. Panigrahi, « Review of Condition Monitoring of Rolling Element Bearing Using Vibration Analysis and Other Techniques », J. Vib. Eng. Technol., vol. 7, no 4, p. 407-414, août 2019, doi: 10.1007/s42417-019-00119-y.

[7] M. R. Mehrjou, N. Mariun, M. Hamiruce Marhaban, et N. Misron, « Rotor fault condition monitoring techniques for squirrel-cage induction machine—A review », Mechanical Systems and Signal Processing, vol. 25, no 8, p. 2827-2848, nov. 2011, doi: 10.1016/j.ymssp.2011.05.007.

[8] Z. Duan, T. Wu, S. Guo, T. Shao, R. Malekian, et Z. Li, « Development and trend of condition monitoring and fault diagnosis of multi-sensors information fusion for rolling bearings: a review », Int J Adv Manuf Technol, vol. 96, no 1-4, p. 803-819, avr. 2018, doi: 10.1007/s00170-017-1474-8.

[9] A. Bhattacharya et P. K. Dan, « Recent trend in condition monitoring for equipment fault diagnosis », Int J Syst Assur Eng Manag, vol. 5, no 3, p. 230-244, sept. 2014, doi: 10.1007/s13198-013-0151-z.

[10] Z. GHEMARI, « Modélisation, simulation et analyse expérimentale du capteur de vibration (accéléromètre) », UNIVERSITE BADJI MOKHTAR – ANNABA, Annaba, Algérie, 2013.

[11] K. S. Gaeid, R. A. Maher, et A. J. Lazim, « Multilevel Inverter Fault-Tolerant Control with Wavelet Index in Induction Motor », J. Electr. Eng. Technol., vol. 14, no 3, p. 1179-1191, mai 2019, doi: 10.1007/s42835-019-00086-0.

[12] N. Haouem, S. Bouras, A. Bouras, et R. Chemes Eddine, « Experimental investigation for the detection of high-risk external electrical faults through stator current analysis », Australian Journal of Electrical and Electronics Engineering, vol. 16, p. 1-10, avr. 2019, doi: 10.1080/1448837X.2019.1604605.

[13] N. Lahouasnia, M. F. Rachedi, D. Drici, et S. Saad, « Load Unbalance Detection Improvement in Three-Phase Induction Machine Based on Current Space Vector

Analysis », J. Electr. Eng. Technol., vol. 15, no 3, p. 1205-1216, mai 2020, doi: 10.1007/s42835-020-00403-y.

[14] D. M. Sonje, P. Kundu, et A. Chowdhury, « A Novel Approach for Sensitive Inter-turn Fault Detection in Induction Motor Under Various Operating Conditions », Arab J Sci Eng, vol. 44, no 8, p. 6887-6900, août 2019, doi: 10.1007/s13369-018-03690-w.

[15] X. Zhang, Z. Liu, J. Wang, et J. Wang, « Time–frequency analysis for bearing fault diagnosis using multiple Q-factor Gabor wavelets », ISA Transactions, vol. 87, p. 225-234, avr. 2019, doi: 10.1016/j.isatra.2018.11.033.

[16] B. Belkacemi, S. Saad, Z. Ghemari, F. Zaamouche, et A. Khazzane, « Detection of Induction Motor Improper Bearing Lubrication by Discrete Wavelet Transforms (DWT) Decomposition », I2M, vol. 19, no 5, p. 347-354, nov. 2020, doi: 10.18280/i2m.190504.

[17] H. Huang et al., « An improved empirical wavelet transform method for rolling bearing fault diagnosis », Sci. China Technol. Sci., avr. 2020, doi: 10.1007/s11431-019-1522-1.

[18] X. Chen et Z. Feng, « Induction motor stator current analysis for planetary gearbox fault diagnosis under time-varying speed conditions », Mechanical Systems and Signal Processing, vol. 140, p. 106691, juin 2020, doi: 10.1016/j.ymssp.2020.106691.

[19] D. Liu, W. Cheng, et W. Wen, « Rolling bearing fault diagnosis via STFT and improved instantaneous frequency estimation method », Procedia Manufacturing, vol. 49, p. 166-172, janv. 2020, doi: 10.1016/j.promfg.2020.07.014.

[20] G. Yu, « A Concentrated Time-frequency Analysis Tool for Bearing Fault Diagnosis », sept. 2020.

[21] S. Anbu, A. Thangavelu, et S. D. Ashok, « Fuzzy C-Means Based Clustering and Rule Formation Approach for Classification of Bearing Faults Using Discrete Wavelet Transform », Computation, vol. 7, no 4, p. 54, sept. 2019, doi: 10.3390/computation7040054.

[22] S. Djaballah, K. Meftah, K. Khelil, M. Tedjini, et L. Sedira, « Detection and diagnosis of fault bearing using wavelet packet transform and neural network », Frattura ed Integrità Strutturale, vol. 13, no 49, p. 291-301, juin 2019, doi: 10.3221/IGF-ESIS.49.29.

[23] I. R. Quinde, J. C. Sumba, L. E. Ochoa, A. Jr. V. Guevara, et R. Morales-Menendez, « Bearing Fault Diagnosis Based on Optimal Time-Frequency Representation Method », IFAC-PapersOnLine, vol. 52, no 11, p. 194-199, 2019, doi: 10.1016/j.ifacol.2019.09.140.

[24] M. Singh et A. G. Shaik, « Faulty bearing detection, classification and location in a three-phase induction motor based on Stockwell transform and support vector machine », Measurement, vol. 131, p. 524-533, janv. 2019, doi: 10.1016/j.measurement.2018.09.013.

[25] M. A. Tajeddini, A. Aalipour, et B. Safarinejadian, « Decision Fusion Method for Bearing Faults Classification Based on Wavelet Denoising and Dempster–Shafer

Theory », Iran J Sci Technol Trans Electr Eng, vol. 43, no 2, p. 295-305, juin 2019, doi: 10.1007/s40998-018-0084-2.

[26] I. Attoui, B. Oudjani, N. Boutasseta, N. Fergani, M.-S. Bouakkaz, et A. Bouraiou, « Novel predictive features using a wrapper model for rolling bearing fault diagnosis based on vibration signal analysis », Int J Adv Manuf Technol, vol. 106, no 7-8, p. 3409-3435, févr. 2020, doi: 10.1007/s00170-019-04729-4.

[27] N. Gharesi, M. M. Arefi, R. Razavi-Far, J. Zarei, et S. Yin, « A neuro-wavelet based approach for diagnosing bearing defects », Advanced Engineering Informatics, vol. 46, p. 101172, oct. 2020, doi: 10.1016/j.aei.2020.101172.

[28] P. Agrawal et P. Jayaswal, « Diagnosis and Classifications of Bearing Faults Using Artificial Neural Network and Support Vector Machine », J. Inst. Eng. India Ser. C, vol. 101, no 1, p. 61-72, févr. 2020, doi: 10.1007/s40032-019-00519-9.

[29] H. Tao, P. Wang, Y. Chen, V. Stojanovic, et H. Yang, « An unsupervised fault diagnosis method for rolling bearing using STFT and generative neural networks », Journal of the Franklin Institute, vol. 357, no 11, p. 7286-7307, juill. 2020, doi: 10.1016/j.jfranklin.2020.04.024.

[30] Y. Zhang, K. Xing, R. Bai, D. Sun, et Z. Meng, « An enhanced convolutional neural network for bearing fault diagnosis based on time–frequency image », Measurement, vol. 157, p. 107667, juin 2020, doi: 10.1016/j.measurement.2020.107667.

[31] M. Zhao, B. Tang, L. Deng, et M. Pecht, « Multiple wavelet regularized deep residual networks for fault diagnosis », Measurement, vol. 152, p. 107331, févr. 2020, doi: 10.1016/j.measurement.2019.107331.

[32] F. de Coulon et J. Neirynck, Théorie et traitement des signaux, 3e éd. rev. et Corr. in Traité d'électricité de l'Ecole polytechnique fédérale de Lausanne, no. 6. Lausanne [Paris]: Presses polytechniques et universitaires romandes [diff. Tec et doc], 1996.

[33] B. Decoux, « Traitement du Signal Déterministe ». Consulté le: 29 juin 2022. [En ligne]. Disponible sur: http://benoit.decoux.free.fr/ENSEIGNEMENT/SIGNAL/CNAM/signal_cnam.html

[34] S. Djaballah, « Etude et optimisation de la transformée en ondelettes pour la détection des défauts dans les roulements », Université Mohamed Chérif Messaâdia, Souk-Ahras.

[35] I. Khelf, « DIAGNOSTIC DES MACHINES TOURNANTES PAR LES TECHNIQUES DE L'INTELLIGENCE ARTIFICIELLE », UNIVERSITE BADJ MOKHTAR, Annaba, 2014.

[36] Y. Yang, Z. Peng, W. Zhang, et G. Meng, « Parameterised time-frequency analysis methods and their engineering applications: A review of recent advances », Mechanical Systems and Signal Processing, vol. 119, p. 182-221, mars 2019, doi: 10.1016/j.ymssp.2018.07.039.

[37] J. Antoni, « Fast computation of the kurtogram for the detection of transient faults », Mechanical Systems and Signal Processing, vol. 21, no 1, p. 108-124, janv. 2007, doi: 10.1016/j.ymssp.2005.12.002.

[38] M.-E.-A. Khodja, A. F. Aimer, A. H. Boudinar, N. Benouzza, et A. Bendiabdellah, « Bearing Fault Diagnosis of a PWM Inverter Fed-Induction Motor Using an Improved Short Time Fourier Transform », J. Electr. Eng. Technol., vol. 14, no 3, p. 1201-1210, mai 2019, doi: 10.1007/s42835-019-00096-y.

[39] I. Atoui, R. Boulkroune, A. Grid, et R. Saidi, « Combination between STFT and DWT for Fault Detection and Diagnosis in Rotating Machinery by Vibration Monitoring », p. 6, 2013.

[40] W. BENTRAH, « Analyse Fréquentielle Par Les Ondelettes Pour Le Diagnostic Des Systèmes Dynamiques », Université Mohamed Khider, Biskra, 2019.

[41] S. A.-E. El-Gindy et al., « Detection of Abnormal Activities from Various Signals Based on Statistical Analysis », Wireless Pers Commun, vol. 125, no 2, p. 1013-1046, juill. 2022, doi: 10.1007/s11277-022-09565-6.

[42] L. Nacib, « DIAGNOSTIC DES DÉFAUTS DANS LES MACHINES TOURNANTES PAR L'ANALYSE VIBRATOIRE », Badji Mokhtar, Annaba, 2015.

[43] Y. Wei, M. Li, W. Xu, et Huang, « A Review of Early Fault Diagnosis Approaches and Their Applications in Rotating Machinery », Entropy, vol. 21, no 4, p. 409, avr. 2019, doi: 10.3390/e21040409.

[44] H. Bae, Y.-T. Kim, S.-H. Lee, S. Kim, et M. H. Lee, « Fault diagnostic of induction motors for equipment reliability and health maintenance based upon Fourier and wavelet analysis », Artif Life Robotics, vol. 9, no 3, p. 112-116, juill. 2005, doi: 10.1007/s10015-004-0331-7.

[45] M. Bahoura et Y. Simard, « Blue whale calls classification using short-time Fourier and wavelet packet transforms and artificial neural network », Digital Signal Processing, vol. 20, no 4, p. 1256-1263, juill. 2010, doi: 10.1016/j.dsp.2009.10.024.

[46] K. Suzuki, Éd., Artificial Neural Networks - Methodological Advances and Biomedical Applications. InTech, 2011. doi: 10.5772/644.

[47] P. H. Sydenham et R. Thorn, Éd., Handbook of measuring system design. Chichester, England: Wiley, 2005.

[48] O. I. Abiodun, A. Jantan, A. E. Omolara, K. V. Dada, N. A. Mohamed, et H. Arshad, « State-of-the-art in artificial neural network applications: A survey », Heliyon, vol. 4, no 11, p. e00938, nov. 2018, doi: 10.1016/j.heliyon.2018.e00938.

[49] S. Dey, N. M. Reang, P. K. Das, et M. Deb, « Comparative study using RSM and ANN modelling for performance-emission prediction of CI engine fuelled with bio-diesohol blends: A fuzzy optimization approach », Fuel, vol. 292, p. 120356, mai 2021, doi: 10.1016/j.fuel.2021.120356.

[50] R. A. Saeed, A. N. Galybin, et V. Popov, « 3D fluid–structure modelling and vibration analysis for fault diagnosis of Francis turbine using multiple ANN and multiple ANFIS », Mechanical Systems and Signal Processing, vol. 34, no 1-2, p. 259-276, janv. 2013, doi: 10.1016/j.ymssp.2012.08.004.

[51] S. Taheri, G. Brodie, et D. Gupta, « Optimised ANN and SVR models for online prediction of moisture content and temperature of lentil seeds in a microwave fluidised bed dryer », Computers and Electronics in Agriculture, vol. 182, p. 106003, mars 2021, doi: 10.1016/j.compag.2021.106003.

[52] H. D. Block, « The Perceptron: A Model for Brain Functioning. I », Rev. Mod. Phys., vol. 34, no 1, p. 123-135, janv. 1962, doi: 10.1103/RevModPhys.34.123.

[53] H. Ramchoun, M. Amine, J. Idrissi, Y. Ghanou, et M. Ettaouil, « Multilayer Perceptron: Architecture Optimization and Training », IJIMAI, vol. 4, no 1, p. 26, 2016, doi: 10.9781/ijimai.2016.415.

[54] A. Malik, A. Kumar, P. Rai, et A. Kuriqi, « Prediction of Multi-Scalar Standardized Precipitation Index by Using Artificial Intelligence and Regression Models », Climate, vol. 9, no 2, p. 28, févr. 2021, doi: 10.3390/cli9020028.

[55] A. Bors, « Introduction of the Radial Basis Function (RBF) Networks », vol. 1, 2001, p. 1-7.

[56] H. Seridi, « Classification et reconnaissance des formes par algorithmes hybrides », Thèse de Doctorat, Université 08 Mai 1945, Guelma, 2009.

[57] I. N. Da Silva, D. Hernane Spatti, R. Andrade Flauzino, L. H. B. Liboni, et S. F. Dos Reis Alves, « The ADALINE Network and Delta Rule », in Artificial Neural Networks, Cham: Springer International Publishing, 2017, p. 41-54. doi: 10.1007/978-3-319-43162-8_4.

[58] A. Ajit, K. Acharya, et A. Samanta, « A Review of Convolutional Neural Networks », in 2020 International Conference on Emerging Trends in Information Technology and Engineering (ic-ETITE), Vellore, India: IEEE, févr. 2020, p. 1-5. doi: 10.1109/ic-ETITE47903.2020.049.

[59] B. Mohebali, A. Tahmassebi, A. Meyer-Baese, et A. H. Gandomi, « Probabilistic neural networks », in Handbook of Probabilistic Models, Elsevier, 2020, p. 347-367. doi: 10.1016/B978-0-12-816514-0.00014-X.

[60] I. A. Basheer et M. Hajmeer, « Artificial neural networks: fundamentals, computing, design, and application », Journal of Microbiological Methods, vol. 43, no 1, p. 3-31, déc. 2000, doi: 10.1016/S0167-7012(00)00201-3.

[61] D. Goyal, A. Choudhary, B. S. Pabla, et S. S. Dhami, « Support vector machines based non-contact fault diagnosis system for bearings », J Intell Manuf, vol. 31, no 5, p. 1275-1289, juin 2020, doi: 10.1007/s10845-019-01511-x.

[62] M. K. Pradhan, « Fault Detection Using Vibration Signal Analysis Of Rolling Element Bearing In Time Domain using an Innovative Time Scalar Indicator », IJMR, vol. 12, no 3, p. 1, 2017, doi: 10.1504/IJMR.2017.10006345.

[63] A. R. Bhende, G. K. Awari, et S. P. Untawale, « Comprehensive bearing condition monitoring algorithm for incipient fault detection using acoustic emission », p. 30, 2014.

[64] R. M. Vogel et N. M. Fennessey, « L moment diagrams should replace product moment diagrams », Water Resour. Res., vol. 29, no 6, p. 1745-1752, juin 1993, doi: 10.1029/93WR00341.

[65] R. Valbuena, M. Maltamo, L. Mehtätalo, et P. Packalen, « Key structural features of Boreal forests may be detected directly using L-moments from airborne lidar data », Remote Sensing of Environment, vol. 194, p. 437-446, juin 2017, doi: 10.1016/j.rse.2016.10.024.

[66] S. Liu, S. Hou, K. He, et W. Yang, « L-Kurtosis and its application for fault detection of rolling element bearings », Measurement, vol. 116, p. 523-532, févr. 2018, doi: 10.1016/j.measurement.2017.11.049.

[67] O. V. Thorsen et M. Dalva, « Failure identification and analysis for high voltage induction motors in petrochemical industry », in Conference Record of 1998 IEEE Industry Applications Conference. Thirty-Third IAS Annual Meeting (Cat. No.98CH36242), St. Louis, MO, USA: IEEE, 1998, p. 291-298. doi: 10.1109/IAS.1998.732309.

[68] « Report of Large Motor Reliability Survey of Industrial and Commercial Installations, Part II », IEEE Trans. on Ind. Applicat., vol. IA-21, no 4, p. 865-872, 1985, doi: 10.1109/TIA.1985.349533.

[69] S. M. Pincus, « Approximate entropy as a measure of system complexity. », Proc. Natl. Acad. Sci. U.S.A., vol. 88, no 6, p. 2297-2301, mars 1991, doi: 10.1073/pnas.88.6.2297.

[70] S. Sassi, B. Badri, et M. Thomas, « Tracking Surface Degradation of Ball Bearings by Means of New Time Domain Scalar Indicators », p. 13.

[71] S. A. Adewusi et B. O. Al-Bedoor, « WAVELET ANALYSIS OF VIBRATION SIGNALS OF AN OVERHANG ROTOR WITH A PROPAGATING TRANSVERSE CRACK », Journal of Sound and Vibration, vol. 246, no 5, p. 777-793, oct. 2001, doi: 10.1006/jsvi.2000.3611.

[72] C. Shen, D. Wang, F. Kong, et P. W. Tse, « Fault diagnosis of rotating machinery based on the statistical parameters of wavelet packet paving and a generic support vector regressive classifier », Measurement, vol. 46, no 4, p. 1551-1564, mai 2013, doi: 10.1016/j.measurement.2012.12.011.

[73] B. Liu, « Selection of wavelet packet basis for rotating machinery fault diagnosis », Journal of Sound and Vibration, vol. 284, no 3-5, p. 567-582, juin 2005, doi: 10.1016/j.jsv.2004.06.047.

[74] X. Wang, V. Makis, et M. Yang, « A wavelet approach to fault diagnosis of a gearbox under varying load conditions », Journal of Sound and Vibration, vol. 329, no 9, p. 1570-1585, avr. 2010, doi: 10.1016/j.jsv.2009.11.010.

[75] Y. Yu, YuDejie, et C. Junsheng, « A roller bearing fault diagnosis method based on EMD energy entropy and ANN », Journal of Sound and Vibration, vol. 294, no 1-2, p. 269-277, juin 2006, doi: 10.1016/j.jsv.2005.11.002.

[76] Y. Li, M. Xu, R. Wang, et W. Huang, « A fault diagnosis scheme for rolling bearing based on local mean decomposition and improved multiscale fuzzy entropy », Journal of Sound and Vibration, vol. 360, p. 277-299, janv. 2016, doi: 10.1016/j.jsv.2015.09.016.

[77] Y. Li, M. Xu, Y. Wei, et W. Huang, « A new rolling bearing fault diagnosis method based on multiscale permutation entropy and improved support vector machine based binary tree », Measurement, vol. 77, p. 80-94, janv. 2016, doi: 10.1016/j.measurement.2015.08.034.

[78] R. Dubey et D. Agrawal, « Bearing fault classification using ANN- based Hilbert footprint analysis », IET Science, Measurement & Technology, vol. 9, no 8, p. 1016-1022, nov. 2015, doi: 10.1049/iet-smt.2015.0026.

[79] I. Attoui, N. Fergani, N. Boutasseta, B. Oudjani, et A. Deliou, « A new time–frequency method for identification and classification of ball bearing faults », Journal of Sound and Vibration, vol. 397, p. 241-265, juin 2017, doi: 10.1016/j.jsv.2017.02.041.

[80] Anbu, Thangavelu, et Ashok, « Fuzzy C-Means Based Clustering and Rule Formation Approach for Classification of Bearing Faults Using Discrete Wavelet Transform », Computation, vol. 7, no 4, p. 54, sept. 2019, doi: 10.3390/computation7040054.

[81] M. Gan, C. Wang, et C. Zhu, « Construction of hierarchical diagnosis network based on deep learning and its application in the fault pattern recognition of rolling element bearings », Mechanical Systems and Signal Processing, vol. 72-73, p. 92-104, mai 2016, doi: 10.1016/j.ymssp.2015.11.014.

[82] G. P. Sillitto, « Interrelations Between Certain Linear Systematic Statistics of Samples from Any Continuous Population », Biometrika, vol. 38, no 3/4, p. 377, déc. 1951, doi: 10.2307/2332583.

[83] H. Liu et Z. Shi, « A Fault Detection Approach Using Variational Mode Decomposition, L-kurtosis and Random Decrement Technique for Rotating Machinery », IJMEA, vol. 8, no 1, p. 16, 2020, doi: 10.11648/j.ijmea.20200801.13.

[84] Q. Gao et J. Xiang, « A Method Using EEMD and L-Kurtosis to Detect Faults in Roller Bearings », in 2018 Prognostics and System Health Management Conference (PHM-Chongqing), Chongqing: IEEE, oct. 2018, p. 71-76. doi: 10.1109/PHM-Chongqing.2018.00018.

[85] H. Liu et J. Xiang, « A Strategy Using Variational Mode Decomposition, L-Kurtosis and Minimum Entropy Deconvolution to Detect Mechanical Faults », IEEE Access, vol. 7, p. 70564-70573, 2019, doi: 10.1109/ACCESS.2019.2920064.

[86] W. Bao, X. Tu, Y. Hu, et F. Li, « Envelope Spectrum L-Kurtosis and Its Application for Fault Detection of Rolling Element Bearings », IEEE Trans. Instrum. Meas., vol. 69, no 5, p. 1993-2002, mai 2020, doi: 10.1109/TIM.2019.2917982.

[87] S. Liu, S. Hou, K. He, et W. Yang, « L-Kurtosis and its application for fault detection of rolling element bearings », Measurement, vol. 116, p. 523-532, févr. 2018, doi: 10.1016/j.measurement.2017.11.049.

[88] A. Ming, W. Zhang, C. Fu, Y. Yang, F. Chu, et Y. Liu, « L-kurtosis-based optimal wavelet filtering and its application to fault diagnosis of rolling element bearings », Journal of Vibration and Control, p. 107754632311658, avr. 2023, doi: 10.1177/10775463231165816.

[89] Y. Li, Y. Yang, X. Wang, B. Liu, et X. Liang, « Early fault diagnosis of rolling bearings based on hierarchical symbol dynamic entropy and binary tree support vector machine », Journal of Sound and Vibration, vol. 428, p. 72-86, août 2018, doi: 10.1016/j.jsv.2018.04.036.

[90] I. Attoui, B. Oudjani, N. Boutasseta, N. Fergani, M.-S. Bouakkaz, et A. Bouraiou, « Novel predictive features using a wrapper model for rolling bearing fault diagnosis based on vibration signal analysis », Int J Adv Manuf Technol, vol. 106, no 7-8, p. 3409-3435, févr. 2020, doi: 10.1007/s00170-019-04729-4.

[91] N. Gharesi, M. M. Arefi, R. Razavi-Far, J. Zarei, et S. Yin, « A neuro-wavelet based approach for diagnosing bearing defects », Advanced Engineering Informatics, vol. 46, p. 101172, oct. 2020, doi: 10.1016/j.aei.2020.101172.

[92] X. Wen, G. Lu, J. Liu, et P. Yan, « Graph modeling of singular values for early fault detection and diagnosis of rolling element bearings », Mechanical Systems and Signal Processing, vol. 145, p. 106956, nov. 2020, doi: 10.1016/j.ymssp.2020.106956.

[93] Z. Chen, A. Mauricio, W. Li, et K. Gryllias, « A deep learning method for bearing fault diagnosis based on Cyclic Spectral Coherence and Convolutional Neural Networks », Mechanical Systems and Signal Processing, vol. 140, p. 106683, juin 2020, doi: 10.1016/j.ymssp.2020.106683.

[94] A. S. Minhas, P. K. Kankar, N. Kumar, et S. Singh, « Bearing fault detection and recognition methodology based on weighted multiscale entropy approach », Mechanical Systems and Signal Processing, vol. 147, p. 107073, janv. 2021, doi: 10.1016/j.ymssp.2020.107073.

[95] F. Safara, S. Doraisamy, A. Azman, A. Jantan, et A. R. Abdullah Ramaiah, « Multi-level basis selection of wavelet packet decomposition tree for heart sound classification », Computers in Biology and Medicine, vol. 43, no 10, p. 1407-1414, oct. 2013, doi: 10.1016/j.compbiomed.2013.06.016.

[96] J. R. M. HOSKINGt et I. ResearchDivision, « L-momentsA: nalysisand Estimationof Distributionus singLinear Combinationsof OrderStatistics », p. 22.

[97] H. Zhu, Z. He, J. Wei, J. Wang, et H. Zhou, « Bearing Fault Feature Extraction and Fault Diagnosis Method Based on Feature Fusion », Sensors, vol. 21, no 7, p. 2524, avr. 2021, doi: 10.3390/s21072524.

[98] D. Goyal, A. Choudhary, B. S. Pabla, et S. S. Dhami, « Support vector machines based non-contact fault diagnosis system for bearings », J Intell Manuf, vol. 31, no 5, p. 1275-1289, juin 2020, doi: 10.1007/s10845-019-01511-x.

[99] K. N. Ravikumar, S. S. Aralikatti, H. Kumar, G. N. Kumar, et K. V. Gangadharan, « Fault diagnosis of antifriction bearing in internal combustion engine gearbox using data mining techniques », Int J Syst Assur Eng Manag, vol. 13, no 3, p. 1121-1134, juin 2022, doi: 10.1007/s13198-021-01407-1.

[100] S. K. Gundewar et P. V. Kane, « Rolling element bearing fault diagnosis using supervised learning methods- artificial neural network and discriminant classifier », Int J Syst Assur Eng Manag, vol. 13, no 6, p. 2876-2894, déc. 2022, doi: 10.1007/s13198-022-01757-4.

[101] M. Behim, L. Merabet, et S. Salah, « Neural Network and L-kurtosis for Diagnosing Rolling Element Bearing Faults », J. Electr. Eng. Technol., mars 2024, doi: 10.1007/s42835-023-01719-1.

[102] Q. Gao et J. Xiang, « A Method Using EEMD and L-Kurtosis to Detect Faults in Roller Bearings », in 2018 Prognostics and System Health Management Conference (PHM-Chongqing), Chongqing: IEEE, oct. 2018, p. 71-76. doi: 10.1109/PHM-Chongqing.2018.00018.

[103] H. Liu et J. Xiang, « A Strategy Using Variational Mode Decomposition, L-Kurtosis and Minimum Entropy Deconvolution to Detect Mechanical Faults », IEEE Access, vol. 7, p. 70564-70573, 2019, doi: 10.1109/ACCESS.2019.2920064.

[104] W. Bao, X. Tu, Y. Hu, et F. Li, « Envelope Spectrum L-Kurtosis and Its Application for Fault Detection of Rolling Element Bearings », IEEE Trans. Instrum. Meas., vol. 69, no 5, p. 1993-2002, mai 2020, doi: 10.1109/TIM.2019.2917982.

[105] S. Nandi, H. A. Toliyat, et X. Li, « Condition Monitoring and Fault Diagnosis of Electrical Motors—A Review », IEEE Trans. On Energy Conversion, vol. 20, no 4, p. 719-729, déc. 2005, doi: 10.1109/TEC.2005.847955.

[106] A. Bellini, F. Filippetti, C. Tassoni, et G.-A. Capolino, « Advances in Diagnostic Techniques for Induction Machines », IEEE Trans. Ind. Electron., vol. 55, no 12, p. 4109-4126, déc. 2008, doi: 10.1109/TIE.2008.2007527.

[107] M. Xu et R. Marangoni, « Vibration Analysis Of A Motor-Flexible Coupling-Rotor System Subject To Misalignment And Unbalance, Part I: Theoretical Model And Analysis », Journal of Sound and Vibration, vol. 176, p. 663-679, oct. 1994, doi: 10.1006/jsvi.1994.1405.

[108] R. R. Obaid et T. G. Habetler, « Effect of load on detecting mechanical faults in small induction motors », in 4th IEEE International Symposium on Diagnostics for Electric

Machines, Power Electronics and Drives, 2003. SDEMPED 2003., Atlanta, GA,USA: IEEE, 2003, p. 307-311. doi: 10.1109/DEMPED.2003.1234591.

[109] P. Gangsar et R. Tiwari, « Signal based condition monitoring techniques for fault detection and diagnosis of induction motors: A state-of-the-art review », Mechanical Systems and Signal Processing, vol. 144, p. 106908, oct. 2020, doi: 10.1016/j.ymssp.2020.106908.

[110] M. Behim, L. Merabet, et S. Saad, « Time - frequency method and artificial neural network classifier for induction motor drive system defects classification », Diagnostyka, p. 1-11, janv. 2024, doi: 10.29354/diag/181192.